Epigenetic Profiles Distinguish Malignant Pleural Mesothelioma from Lung Adenocarcinoma

Yasuhiro Goto,[1] Keiko Shinjo,[1,3] Yutaka Kondo,[1] Lanlan Shen,[7] Minoru Toyota,[8] Hiromu Suzuki,[9] Wentao Gao,[10] Byonggu An,[1] Makiko Fujii,[1] Hideki Murakami,[1] Hirotaka Osada,[1,3] Tetsuo Taniguchi,[5] Noriyasu Usami,[5] Masashi Kondo,[4] Yoshinori Hasegawa,[4] Kaoru Shimokata,[11] Keitaro Matsuo,[2] Toyoaki Hida,[6] Nobukazu Fujimoto,[12] Takumi Kishimoto,[12] Jean-Pierre J. Issa,[7] and Yoshitaka Sekido[1,3]

Divisions of [1]Molecular Oncology and [2]Epidemiology and Prevention, Aichi Cancer Center Research Institute; Departments of [3]Cancer Genetics and [4]Respiratory Medicine and [5]Division of General Thoracic Surgery, Nagoya University Graduate School of Medicine; [6]Department of Thoracic Oncology, Aichi Cancer Center Hospital, Nagoya, Japan; [7]Department of Leukemia, The University of Texas M. D. Anderson Cancer Center, Houston, Texas; [8]Department of Biochemistry and [9]First Department of Internal Medicine, Sapporo Medical University, Sapporo, Japan; [10]Department of General Surgery, First Affiliated Hospital of Nanjing Medical University, Nanjing, China; [11]Department of Biomedical Sciences, Chubu University, Kasugai, Japan; and [12]Department of Respiratory Medicine, Okayama Rosai Hospital, Okayama, Japan

Abstract

Malignant pleural mesothelioma (MPM) is a fatal thoracic malignancy, the epigenetics of which are poorly defined. We performed high-throughput methylation analysis covering 6,157 CpG islands in 20 MPMs and 20 lung adenocarcinomas. Newly identified genes were further analyzed in 50 MPMs and 56 adenocarcinomas via quantitative methylation-specific PCR. Targets of histone H3 lysine 27 trimethylation (H3K27me3) and genetic alterations were also assessed in MPM cells by chromatin immunoprecipitation arrays and comparative genomic hybridization arrays. An average of 387 genes (6.3%) and 544 genes (8.8%) were hypermethylated in MPM and adenocarcinoma, respectively. Hierarchical cluster analysis showed that the two malignancies have characteristic DNA methylation patterns, likely a result of different pathologic processes. In MPM, a separate subset of genes was silenced by H3K27me3 and could be reactivated by treatment with a histone deacetylase inhibitor alone. Integrated analysis of these epigenetic and genetic alterations revealed that only 11% of heterozygously deleted genes were affected by DNA methylation and/or H3K27me3 in MPMs. Among the DNA hypermethylated genes, three (*TMEM30B, KAZALD1*, and *MAPK13*) were specifically methylated only in MPM and could serve as potential diagnostic markers. Interestingly, a subset of MPM cases (4 cases, 20%) had very low levels of DNA methylation and substantially longer survival, suggesting that the epigenetic alterations are one mechanism affecting progression of this disease. Our findings show a characteristic epigenetic profile of MPM and uncover multiple distinct epigenetic abnormalities that lead to the silencing of tumor suppressor genes in MPM and could serve as diagnostic or prognostic targets. [Cancer Res 2009;69(23):9073–82]

Introduction

Malignant pleural mesothelioma (MPM) is an aggressive tumor that has been associated with asbestos exposure (1). Approximately 10,000 to 15,000 patients worldwide are newly diagnosed with MPM annually, and the number of patients is projected to increase over the next two decades in Asia and the United States (1, 2). Although the inhalation of asbestos is a well-known risk factor, the lack of clinical symptoms in the early stages of MPM as well as of useful diagnostic markers makes early diagnosis virtually impossible. In addition to these difficulties, the relative ineffectiveness of available therapies also contributes to the death of MPM patients shortly after diagnosis (1, 3). Therefore, further molecular analysis of MPM is urgently needed to identify effective markers that could be applied to blood or pleural fluid for an early valid diagnosis.

The central mechanisms underlying MPM formation are still unclear. Several genetic abnormalities seem to be involved in MPM, such as a loss of the *p16* locus or mutations in the *NF2* gene (4–6). However, recent whole-transcriptome sequencing approaches as well as comparative genomic hybridization analyses have revealed relatively few genetic mutations in MPM, about six genes per individual MPM (7, 8). The low frequency of genetic abnormalities raises the question of whether alternative mechanisms might also be contributing to the inactivation of genes, leading to tumor formation.

Dysregulation of epigenetic transcriptional control, particularly aberrant promoter DNA methylation and histone modifications, is a fundamental feature of human malignancies (9). The relationship between promoter DNA hypermethylation and inflammation has been documented in many types of cancers, including MPM (10). It could be that asbestos exposure contributes to MPM formation through this relationship (11–14), because it is known that asbestos induces continuous inflammation instead of directly transforming primary human mesothelial cells in tissue culture (15–17). In addition, recent cumulative studies of aberrant DNA methylation in human cancers showed high rates of aberrant promoter methylation in a subset of cancers, termed the CpG island methylator phenotype, which may also be contributing to MPM formation (18). However, there is currently limited information available regarding the DNA methylation status of MPM.

In addition to DNA methylation, a dysregulation of histone H3 lysine 27 trimethylation (H3K27me3) is known to be involved in several human malignancies (19). Enhancer of zeste 2, a polycomb

Note: Supplementary data for this article are available at Cancer Research Online (http://cancerres.aacrjournals.org/).

Y. Goto and K. Shinjo contributed equally to this work.

Requests for reprints: Yutaka Kondo, Division of Molecular Oncology, Aichi Cancer Center Research Institute, 1-1 Kanokoden, Chikusa-ku, Nagoya 464-8681, Japan. Phone: 81-52-764-2993; Fax: 81-52-764-2993; E-mail: ykondo@aichi-cc.jp.

doi:10.1158/0008-5472.CAN-09-1595

group protein part of polycomb repressor complex 2, has histone methyltransferase activity with substrate specificity for H3K27. Because polycomb group–mediated gene silencing is initiated by the histone deacetylase (HDAC) activity of polycomb repressor complex 2, inhibition of HDAC can efficiently reactivate the H3K27me3 target genes (20, 21). However, this epigenetic event has not been studied in MPM.

To investigate aberrant epigenetic events in MPM, we performed global screening for genes with aberrant DNA hypermethylation using the methylated CpG island amplification microarray (MCAM), which provides reproducible results with a high validation rate and successfully detects genes methylated in normal as well as in cancerous tissues (22, 23). We also conducted combined analysis of MCAM, chromatin immunoprecipitation-microarrays, and array comparative genomic hybridization to show the relationship between these epigenetic and genetic abnormalities in MPMs. Our comprehensive analysis revealed that multiple epigenetic abnormalities play important roles in MPM carcinogenesis and may be valid therapeutic targets.

Materials and Methods

Cell lines. Two MPM cell lines [ACC-MESO-1 (MESO1) and Y-MESO-8A (MESO8)] previously established in our laboratory (24) and one nonmalignant mesothelial cell line (MeT-5A) were used for the study. MeT-5A was purchased from the American Type Culture Collection and cultured according to the instructions (CRL-9444). MESO1 and MESO8 were maintained in RPMI 1640 (Sigma-Aldrich) supplemented with 10% fetal bovine serum (Invitrogen) and antibiotic-antimycotic (Invitrogen) at 37°C in a humidified incubator with 5% CO_2.

Tissue samples. Fifty MPM samples, 56 adenocarcinoma samples, 4 normal mesothelial tissues, and 10 normal lung tissues were obtained from Japanese patients at the Aichi Cancer Center Hospital, Nagoya University Hospital, and the affiliated hospitals. Samples and clinical data were collected after appropriate institutional review board approval was received and written informed consent had been obtained from all patients. We scraped the surface of the resected normal lung from lung cancer cases and obtained normal pleural tissues. Normal lung tissues were obtained from the normal lung of lung cancer cases. Histologic and cytologic examination of both normal mesothelial and lung tissues revealed no remarkable findings as malignant tissues. In these normal tissues, no aberrant methylation was detected in five genes with pyrosequencing analysis (Supplementary Table S1).

DNA preparation. Genomic DNA was extracted using a standard phenol-chloroform method. Fully methylated DNA was prepared by treating genomic DNA with *Sss*I methylase (New England Biolabs; ref. 23). Unmethylated DNA was prepared by treating genomic DNA with phi29 DNA polymerase (GenomiPhi DNA Amplification kit; Amersham Biosciences) according to the manufacturer's protocol.

Methylated CpG island amplification-microarray. For MCAM analysis, we analyzed 20 MPMs (average age, 59.1 years; range, 45-78 years) and 20 adenocarcinomas (average age, 62.8 years; range, 44-76 years). A detailed protocol of MCAM has been described previously (22, 23). We used a human custom promoter array (G4497A; Agilent Technologies) containing 15,134 probes corresponding to 6,157 unique genes (23).

Hierarchical clustering analysis. Cluster analysis was done using an agglomerative hierarchical clustering algorithm (23, 25). For specimen clustering, pairwise similarity measures among specimens were calculated using Cluster 3.0 software[13] or Minitab 15 statistical software[14] based on the DNA methylation intensity measurements across all genes.

Methylation analysis. We performed bisulfite treatment as described previously (26, 27). The DNA methylation levels were measured using Pyrosequencing technology. For each assay, the setup included both positive controls (samples after *Sss*I treatment) and negative controls (samples after whole-genome amplification using GenomiPhi V2), with mixing experiments to rule out bias, and repeat experiments to assess reproducibility (28). Conventional methylation-specific PCR (MSP) was also carried out for the *transmembrane protein 30B* (*TMEM30B*), *Kazal-type serine protease inhibitor domain 1* (*KAZALD1*), and *mitogen-activated protein kinase 13* (*MAPK13*) genes. PCR products were visualized on 6% polyacrylamide or 3% agarose gels stained with ethidium bromide. MSP products were subsequently confirmed by bisulfite sequencing analysis. Quantitative MSP was also carried out using SYBR Green (Applied Biosystems). In addition to primers designed specifically for the gene of interest, an internal reference primer set designed for *LINE1*, which can amplify *LINE1* loci irrespective of DNA methylation status, was included in the analysis to normalize for input DNA. The percentage methylated reference is calculated by dividing the GENE:LINE1 ratio of the sample by the GENE:LINE1 ratio of the *Sss*I-treated methylated DNA and multiplying by 100 (29). To determine the cutoff value for the classification of methylated and unmethylated loci, we compared the percentage methylated reference and the methylation level from pyrosequencing analysis in each gene. The best discrimination cutoff values were 7% for *TMEM30B*, 5% for *KAZALD1*, and 5% for *MAPK13*. Primer sequences and PCR conditions are shown in Supplementary Table S2. All of the primers were designed to examine the methylation status of CpGs within 0.5 kb of the transcription start site.

Trichostatin A and 5-aza-2′-deoxycytidine treatment of cells. Cells were treated with 5-aza-2′-deoxycytidine (5Aza-dC; Sigma-Aldrich) or trichostatin A (MP Biomedicals) as described previously (23).

Chromatin immunoprecipitation-microarrays. Chromatin immunoprecipitation was done based on the previously published methods (21, 30). Trimethylated H3K27-specific samples and the input samples were labeled with Cy5 and Cy3, respectively. Labeled chromatin immunoprecipitation products were hybridized to CpG microarray using the same protocol as MCAM. A Cy5/Cy3 signal in excess of 1.5 was considered as an enrichment of H3K27me3 (Supplementary Table S3).

Quantitative reverse transcription-PCR analyses. Total RNA was isolated using Trizol (Invitrogen). RNA (2 μg) was reverse transcribed with MPMLV (Promega). TaqMan quantitative reverse transcription-PCRs and SYBR Green quantitative reverse transcription-PCRs were carried out in triplicate for the target genes (Applied Biosystems). Primer sequences are shown in Supplementary Table S2.

Statistical analysis. Associations between methylation status and clinicopathologic variables were analyzed by the Mann-Whitney *U* test, Fisher's exact test, Kruskal-Wallis test, or a linear regression model. The Kaplan-Meier method was used to estimate overall survival. The Cox proportional hazards models were used for estimation of hazard ratio. All reported *P* values were two-sided, with $P < 0.05$ considered statistically significant. Calculations were carried out with either StatView software version 5.0 (Abacus Concepts) or Stata version 8 (StataCorp).

Results

DNA methylation profiling by MCAM analysis in MPM and adenocarcinoma. To compare the global DNA methylation profiles of MPM and adenocarcinoma, we analyzed 20 samples of each using MCAM. Technical replications of MCAM were done for six cases of MPM and highly reproducible methylation profiles were obtained among the replicates ($R^2 = 0.93$; Supplementary Fig. S1). A Cy5/Cy3 signal in excess of 2.0 in MCAM was considered methylation-positive in a previous study (23). In the present study, 18 randomly selected genes were subsequently assessed by pyrosequencing analysis in MPM and adenocarcinoma samples. A methylation level >15% was considered methylation-positive (23). A high concordance was observed between the methylation status by

[13] http://rana.lbl.gov/EisenSoftware.htm
[14] http://www.minitab.com

MCAM and pyrosequencing analyses (specificity, 90%; sensitivity, 82%; Supplementary Table S4) as was also shown in previous studies (22, 23). We will hereafter consider a signal ratio >2.0 in MCAM as methylation-positive.

In the cohybridization of MCA products from normal mesothelium DNA and normal lung tissue DNA, a high concordance in the methylation status was observed (R^2 = 0.87; Fig. 1*A*), suggesting that tissue-specific methylation is rare in these two tissues.

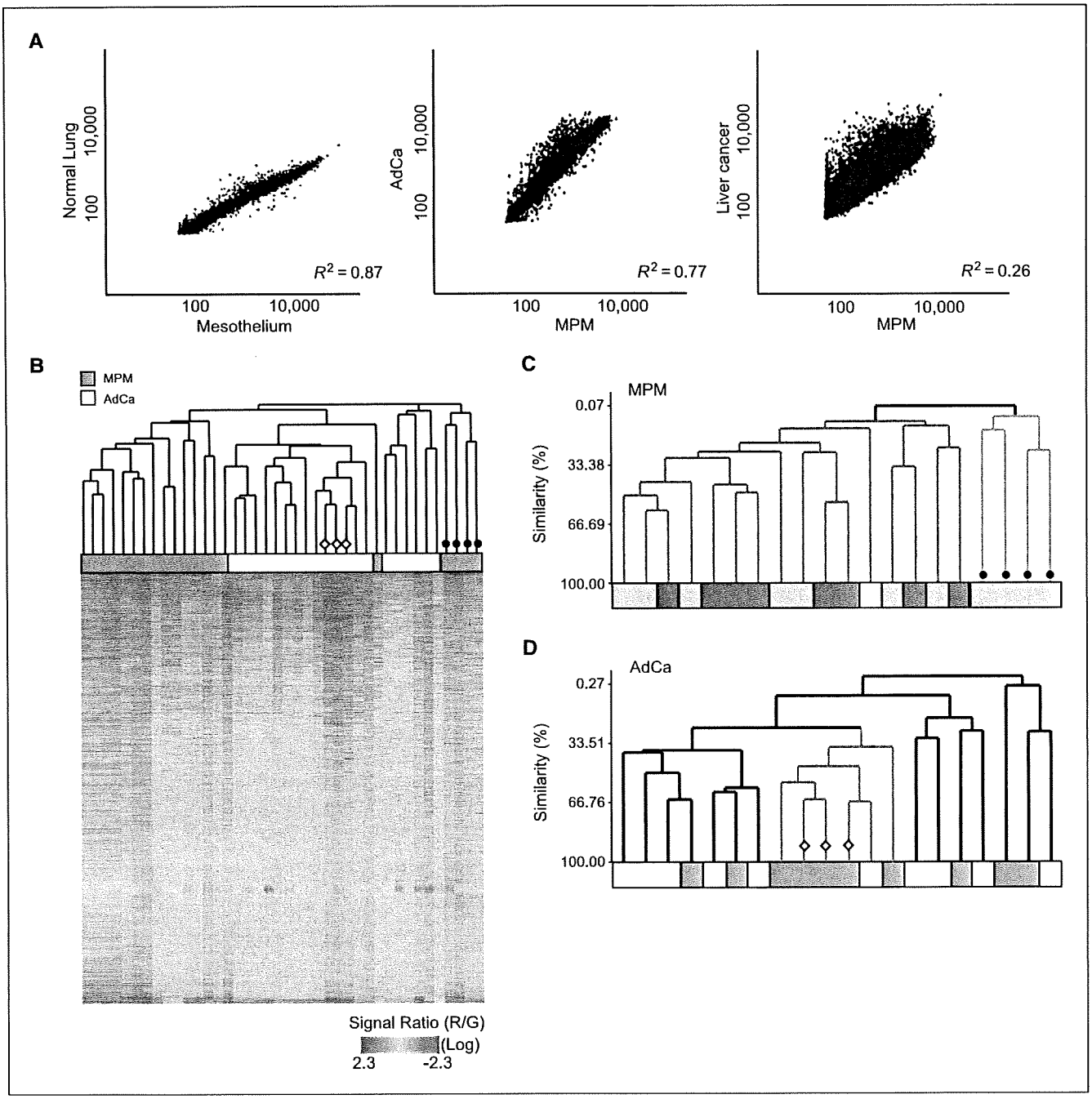

Figure 1. DNA methylation profiling by MCAM analysis. *A*, scatter plot analysis of signal intensity (log scale) between normal mesothelium (mixture of two cases) and normal lung tissue (mixture of four cases; *left*), MPM and adenocarcinoma (*AdCa*; both a mixture of four cases in both tumors; *middle*), and MPM and liver cancer (both a mixture of four cases in both tumors, *right*). The coefficient of determination (R^2) in the linear regression model is indicated in each analysis. *B*, dendrogram and heat-map overview of hierarchical cluster analysis of DNA methylation data from 40 samples (*blue boxes*, MPM; *white boxes*, adenocarcinoma) using all 6,157 genes (*Y axis*). Color corresponds to methylation level as indicated in the $\log_2$-transformed scale bar below the matrix. *Red* and *blue*, high and low levels, respectively; *black circle*, <300 genes methylated in these MPMs; *open diamond*, >950 genes methylated in these adenocarcinomas. *C*, defining subclasses in MPMs using hierarchical clustering. All 6,157 genes were used for the analysis of 20 MPMs. *Y axis*, similarity. Color boxes indicate histologic subtype of MPM. *Yellow*, *green*, *blue*, and *white boxes*, epithelial, biphasic, sarcomatoid, and variants, respectively; *black circle*, same MPMs as in *B*. *D*, subclasses in adenocarcinomas using hierarchical clustering. *Y axis*, similarity. *Gray* and *white boxes*, smokers and nonsmokers, respectively; *open diamond*, same adenocarcinomas as in *B*.

Although ~70% of hypermethylated genes in MPMs were also found to be methylated in adenocarcinoma, a subset of loci were differently methylated in each tumor (R^2 = 0.77; Fig. 1*A*; Supplementary Fig. S2*A*). Interestingly, a larger number of loci were differently methylated in MPM and liver cancer (ref. 23; R^2 = 0.26), suggesting that the methylation profiles of MPM and adenocarcinoma have more in common (Fig. 1*A*).

Unsupervised hierarchical clustering analysis using the methylation status of 6,157 genes showed that adenocarcinomas seemed to be more frequently methylated than MPMs and that a subset of adenocarcinomas was extensively methylated (Fig. 1*B*). The majority of the MPM and adenocarcinoma samples could be classified into distinct subgroups according to DNA methylation status.

DNA methylation status affects clinicopathologic features of MPM and adenocarcinoma. Unsupervised hierarchical clustering analysis of MPMs using the 6,157-gene methylation status indicated two major subgroups, one of which had only the epithelial type of MPMs with less methylation (<300 genes; 4 cases; Fig. 1*C*). This subgroup tended to have longer survival rates than the other (19.5 ± 13.7 versus 14.5 ± 3.3 months; hazard ratio, 0.48; 95% confidence interval, 0.10-2.21; P = 0.3; Supplementary Fig. S3*A*). Interestingly, when we selected 445 genes that are commonly methylated in more than one-third of MPM cases, MPMs could be divided into two groups using this set of genes: high methylation group (n = 8) and low methylation group (n = 10; Supplementary Fig. S3*B*; Supplementary Table S5). Patients with low methylation lived significantly longer (21.6 ± 13.3 months) than those with high methylation (6.8 ± 4.1 months; hazard ratio, 0.16; 95% confidence interval, 0.04-0.63; P < 0.01; Supplementary Fig. S3*C*).

Adenocarcinomas were divided into four subgroups (Fig. 1*D*). One subgroup consisted of six adenocarcinoma samples that had more methylated genes than the other samples (911 ± 220 versus 387 ± 231 genes; P < 0.01) and came mostly from smokers (5 of 6 cases; mean pack-years smoked, 68.6 ± 22.9 years). Smokers had significantly more methylated genes than nonsmokers in adenocarcinoma (728 ± 338 versus 360 ± 206 genes; P = 0.02; Table 1). The majority of methylated genes (82%) in nonsmokers were also methylated in smokers (Supplementary Fig. S2*B*). In contrast, there were numbers of specifically methylated genes in smokers, suggesting that smoking affects DNA methylation in a set of genes.

Asbestos exposure appeared to have little effect on methylation status in MPM (exposure 386 ± 203 genes versus nonexposure 320 ± 118 genes; P = 0.4; Table 1). In addition, >60% of methylated genes in asbestos exposure cases were also methylated in asbestos nonexposure cases and vice versa (Supplementary Fig. S2*C*).

The numbers of methylated genes in stages I and II were significantly fewer than those in stages III and IV in both MPM and adenocarcinoma (P < 0.05), suggesting that DNA methylation increases in frequency as the diseases progress.

Distinct DNA methylation patterns between MPM and adenocarcinoma. Less than 700 genes were methylated in most of the MPMs, with the average being 387 genes (range, 120-755 genes; Fig. 2*A*) compared with 544 genes (range, 133-1,212 genes) in adenocarcinomas. In addition, genes commonly hypermethylated

Table 1. Incidence of hypermethylated genes and clinicopathologic parameters

	MPM		Adenocarcinoma	
	n (%)	No. methylated genes	*n* (%)	No. methylated genes
Age (y)*				
<65	14 (75)	388 ± 193	10 (50)	546 ± 404
≥65	5 (25)	430 ± 212	10 (50)	542 ± 262
Gender				
Female	2 (10)	261 ± 46	8 (40)	395 ± 218
Male	18 (90)	401 ± 202	12 (60)	643 ± 364
Asbestos exposure*				
Exposed	14 (78)	386 ± 203		
Not exposed	4 (22)	320 ± 118		
Histology				
Epithelial	11 (55)	356 ± 208		
Biphasic	7 (35)	403 ± 172		
Sarcomatoid	1 (5)	700		
Variants	1 (5)	297		
Stage*†				
I	1 (6)	211	12 (60)	427 ± 269
II	4 (25)	174 ± 76	4 (20)	748 ± 473
III	6 (38)	394 ± 179	4 (20)	691 ± 259
IV	5 (31)	308 ± 162	0 (0)	
Smoking status*				
Smoker	14 (88)	367 ± 204	10 (50)	728 ± 338‡
Nonsmoker	2 (12)	261	10 (50)	360 ± 206

*Clinical data of some patients were unavailable.
†Number of methylated genes in I and II is significantly smaller than in III and IV in MPMs and adenocarcinomas (P < 0.05).
‡Number of methylated genes in this group is significantly higher (P < 0.05) than in the other group.

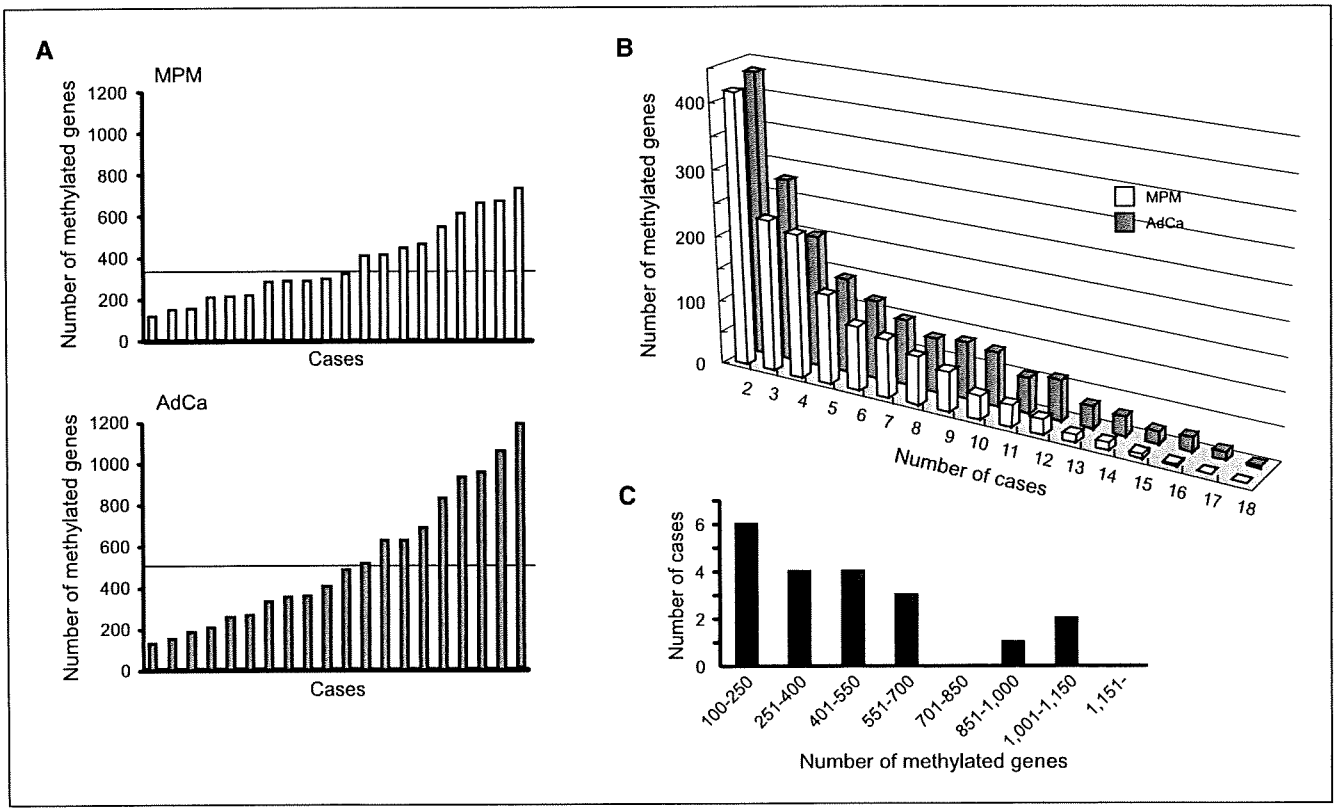

Figure 2. Comparison of distinct DNA methylation patterns between MPM and adenocarcinoma. *A*, number of methylated genes in each case. *Line*, average numbers of methylated genes (387 and 544 genes in MPM and adenocarcinoma, respectively). *B*, number of genes (*Y axis*) that were commonly methylated in *x* number of cases, where *x* is the axis in MPM (*white*) or adenocarcinoma (*gray*). *C*, bimodal distribution of methylated genes out of 1,457 loci in adenocarcinoma. The number of methylated genes (*X axis*) is plotted against the number of cases (*Y axis*).

in >10 MPMs were quite rare (<40 genes), whereas >80 genes were commonly hypermethylated in 10 adenocarcinomas, suggesting that hypermethylated genes vary more in each MPM case ($P < 0.01$; Fig. 2*B*). Notably, analysis of 1,457 genes that were methylated in >2 adenocarcinoma cases showed the bimodal distribution of methylation pattern as shown previously in CpG island methylator phenotype–positive tumor (ref. 31; Fig. 2*C*).

Two epigenetic mechanisms regulating gene expression in MPM cell lines. We next examined the changes in expression of genes identified by MCAM analysis before and after epigenetic treatments (Fig. 3*A*). These genes were methylated to some extent and were silenced in both MPM cell lines, MESO1 and MESO8, in contrast to their high expression levels in normal mesothelial tissue. Each gene in the different cell lines responded differently to the epigenetic treatments. *Ankyrin 1* (*ANK1*) was reactivated by the DNA methyltransferase inhibitor, 5Aza-dC, in a dose-dependent manner but was not reactivated by a HDAC inhibitor trichostatin A alone, which is the typical response to epigenetic treatment in DNA methylation target genes (32). *Progesterone receptor* (*PGR*) was reactivated by both 5Aza-dC and trichostatin A alone regardless of its DNA methylation status. Unexpectedly, the response to trichostatin A treatment in *proenkephalin* (*PENK*) differed between these two cell lines, although the CpG island in both cell lines was densely methylated. These findings, taken together, most likely indicate that another epigenetic mechanism regulates gene expression in MPM cells.

H3K27me3 mediated by polycomb group protein is an alternative silencing mechanism for tumor suppressor genes in human malignancies (19). We examined the H3K27me3 status in the same three genes (Fig. 3*B*). H3K27me3 was enriched in the *PGR* promoter in both cell lines and in the *PENK* promoter in MESO8. No enrichment of H3K27me3 was observed in either the *PENK* promoter in MESO1 or in the *ANK1* promoter in both cell lines that are densely DNA methylated.

Integrated analysis of genetic and epigenetic alterations. To examine H3K27me3 targets and the relation between DNA methylation and H3K27me3 on the CpG promoters in MPM cells, we carried out a chromatin immunoprecipitation-microarray analysis using the same promoter array (Fig. 4*A*). First, we validated the chromatin immunoprecipitation-microarray results by chromatin immunoprecipitation-PCR with randomly selected genes and found good concordance between the two analyses (specificity, 82%; sensitivity, 82%; Supplementary Table S3). We counted the genes that were enriched with H3K27me3 in MESO1 or MESO8 but not enriched in MeT-5A (a nonmalignant mesothelial cell line) and found 113 and 241 target genes in MESO1 and MESO8, respectively (Fig. 4*A*). DNA methylation was more frequently observed than H3K27me3 in the CpG promoters in both cell lines. There was some overlap between DNA-methylated and H3K27me3 target genes; however, the majority of the genes enriched with H3K27me3 revealed no detectable DNA hypermethylation, whereas most genes showing DNA hypermethylation showed no enrichment with H3K27me3. These results suggest that DNA hypermethylation and

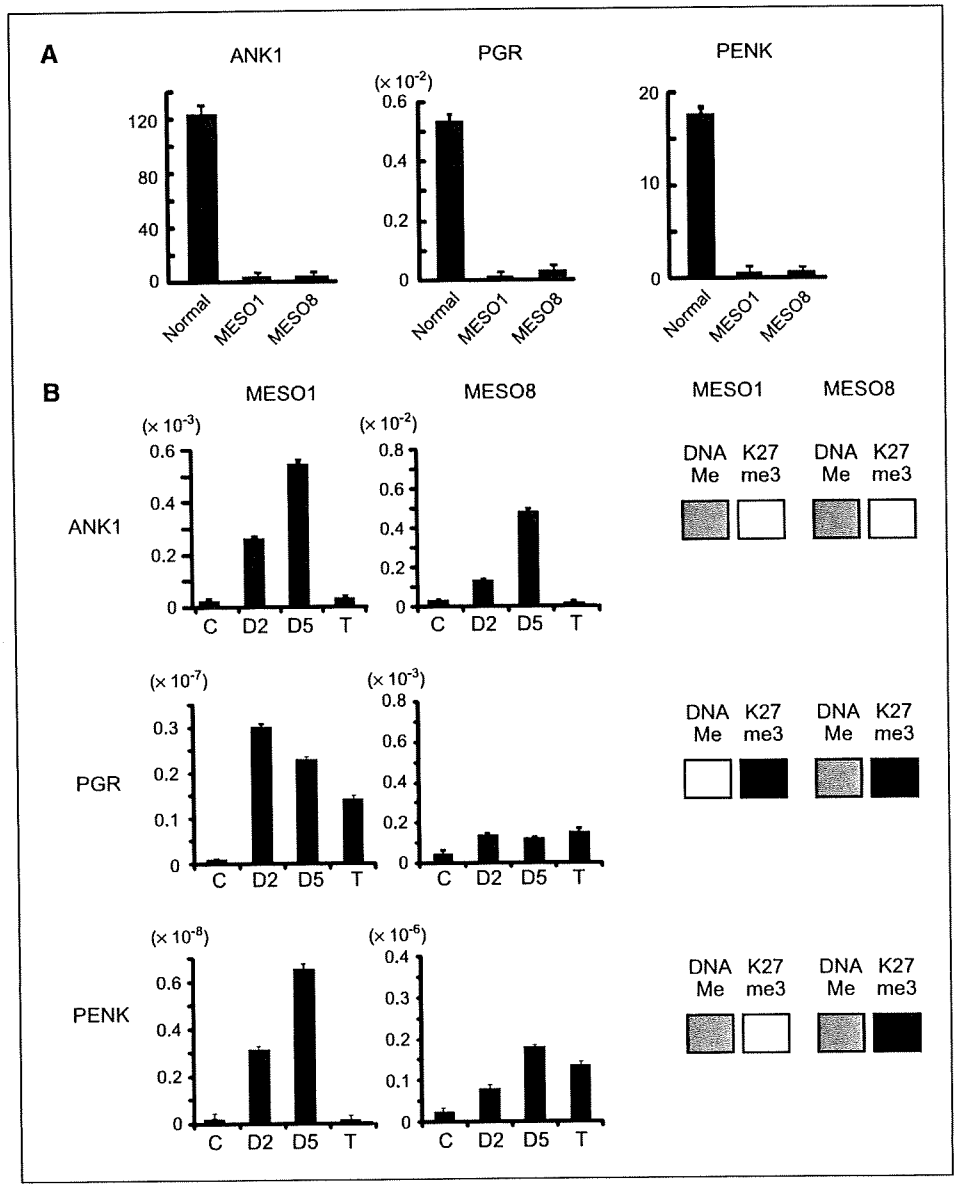

Figure 3. Relationship between gene expression and epigenetic alterations in MPM cell lines. *A*, gene expression was measured by quantitative PCR in normal mesothelial tissue, MESO1, and MESO8. *Y axis*, relative values of mRNA expression for each gene to glyceraldehyde-3-phosphate dehydrogenase. *Bars*, SD from experiments in triplicate. *B*, reactivation of silenced genes by DNA methyltransferase inhibitor (5Aza-dC) or HDAC inhibitor (trichostatin A) in three representative genes. After treatment with either PBS (control; *C*), 2 μmol/L (*D2*) or 5 μmol/L (*D5*) 5Aza-dC, or trichostatin A (*T*), each silenced gene was reactivated. *Y axis*, relative values of mRNA expression for each gene to glyceraldehyde-3-phosphate dehydrogenase. *Right columns*, status of DNA methylation (*DNA Me*) and H3K27me3 (*K27me3*). Regarding levels of DNA methylation in these genes, each gene shows high (*gray*; DNA methylation level >60%) or low (*white*; DNA methylation level <10%) methylation. For H3K27me3, each gene shows enrichment (*black*) or nonenrichment (*white*) of H3K27me3. DNA methylation levels were assayed by pyrosequencing and H3K27me3 status was assayed by chromatin immunoprecipitation-microarray and chromatin immunoprecipitation-PCR.

H3K27me3 may contribute to cancer development through the silencing of specific target genes in MPM cells (Fig. 4*A* and *B*).

We next carried out an integrated genetic and epigenetic analysis using array comparative genomic hybridization data that we have reported previously in the same cell lines (33). A total of 5,746 genes covered by both MCAM and comparative genomic hybridization arrays were analyzed. Genomic deletions were detected in 190 and 565 genes in MESO1 and MESO8, respectively. The majority of those genes showed heterozygous deletions, whereas only 8 and 3 genes showed homozygous deletions in MESO1 and MESO8, respectively (Fig. 4*B*). Twenty-one of 190 (11%, MESO1) and 63 of 565 (11%, MESO8) deleted genes were also affected by DNA methylation or H3K27me3, most of which were affected by heterozygous deletions and DNA methylation. Interestingly, all these three events were observed in one gene in MESO8, *A-kinase anchor protein 12* (*AKAP12*), which has been reported as a tumor suppressor gene and a target of DNA methylation in childhood myeloid malignancies (34). Representative analyses of chromosomes 9 and 10 where two important tumor suppressor genes, *CDKN2A* and *PTEN*, were homozygously deleted, showed that genetic deletion is rare. It was also found that genetic deletion, DNA methylation, and H3K27me3 do not frequently overlap on the same loci in these chromosomes (Fig. 4*C*).

Identification of MPM-specific methylation markers. DNA methylation has been proposed as a powerful potential marker for cancer diagnosis (35). To identify specific methylation markers for MPM, we first selected 8 genes from the MCAM analysis, which were methylation-positive (Cy5/Cy3 > 2.0) in at least four MPMs and methylation-negative in all of the adenocarcinomas (Fig. 5*A*). We validated the genes by MSP and found that three of them, *TMEM30B*, *KAZALD1*, and *MAPK13*, were the best specific methylation markers for MPM (Fig. 5*B* and *C*). In the same set of MPMs analyzed by MCAM, DNA methylation was detected by MSP analysis in 11 (58%), 8 (42%), and 2 (11%) cases of 19 in the *TMEM30B*, *KAZALD1*, and *MAPK13* genes, respectively.

To confirm whether these methylation markers might prove valid in another group of MPM patients, we obtained an additional 31 MPM samples from a different institution. Altogether, the methylation status of these three genes was analyzed in 50 MPMs by quantitative MSP (Fig. 5*D*). DNA methylation occurred in 19 cases (38%) in *TMEM30B*, 24 (48%) in *KAZALD1*, and 19 (38%) in *MAPK13*. In contrast, no substantial DNA methylation was detected in those three genes in 56 adenocarcinomas (Fig. 5*C* and *D*). The sensitivity and specificity of hypermethylation in at least one of the above three genes for a differential diagnosis of MPM from adenocarcinoma were found to be 72% and 100%, respectively. Kaplan-Meier survival analysis on methylation status of these three MPM-specific methylation genes revealed that MPM patients with no methylation tended to have prolonged survival (n = 11; 17.0 ± 13.9 months) compared with those with at least one gene methylated (n = 34; 12.1 ± 7.8 months; hazard ratio, 0.58; 95% confidence interval = 0.26-1.28; P = 0.17; Supplementary Fig. S3*D*).

Discussion

In this study, we analyzed and compared the DNA methylation status of MPM and adenocarcinoma to highlight the methylation profile of MPM. Although normal mesothelium and lung tissue develop from different germ layers (mesoderm and endoderm, respectively), their hypermethylation profiles are very similar (R^2 = 0.87), indicating that tissue-specific methylation differences in these two normal tissues are infrequent. Previous genome-wide methylation analyses of a variety of normal tissues have consistently shown that tissue-specific methylation is quite rare, thus validating our findings (22, 36, 37). By contrast, the differences in hypermethylated genes between MPM and adenocarcinoma were more numerous than in normal tissues, which might be a result of different pathologic processes in the two malignancies.

A previous study of the methylation status of seven loci showed that methylation is less prevalent in MPM than in adenocarcinoma (11). Our own global DNA methylation analysis revealed that hypermethylated genes are less frequent and more varied overall in MPM than in adenocarcinoma. Fewer than 700 genes were methylated in most of the MPMs (average hypermethylated genes, 387 ± 196 genes). This contrasted with a subset of adenocarcinoma samples, all of them from smokers (mean pack-years smoked, 67.3 ± 14.2 years) that were extensively methylated (>950 genes). In adenocarcinoma, smoking seems to be a mechanism driving tumors into distinct epigenetic subclasses. It has been suggested that certain adenocarcinomas can be predisposed to hypermethylation and a phenotype known as CpG island methylator phenotype

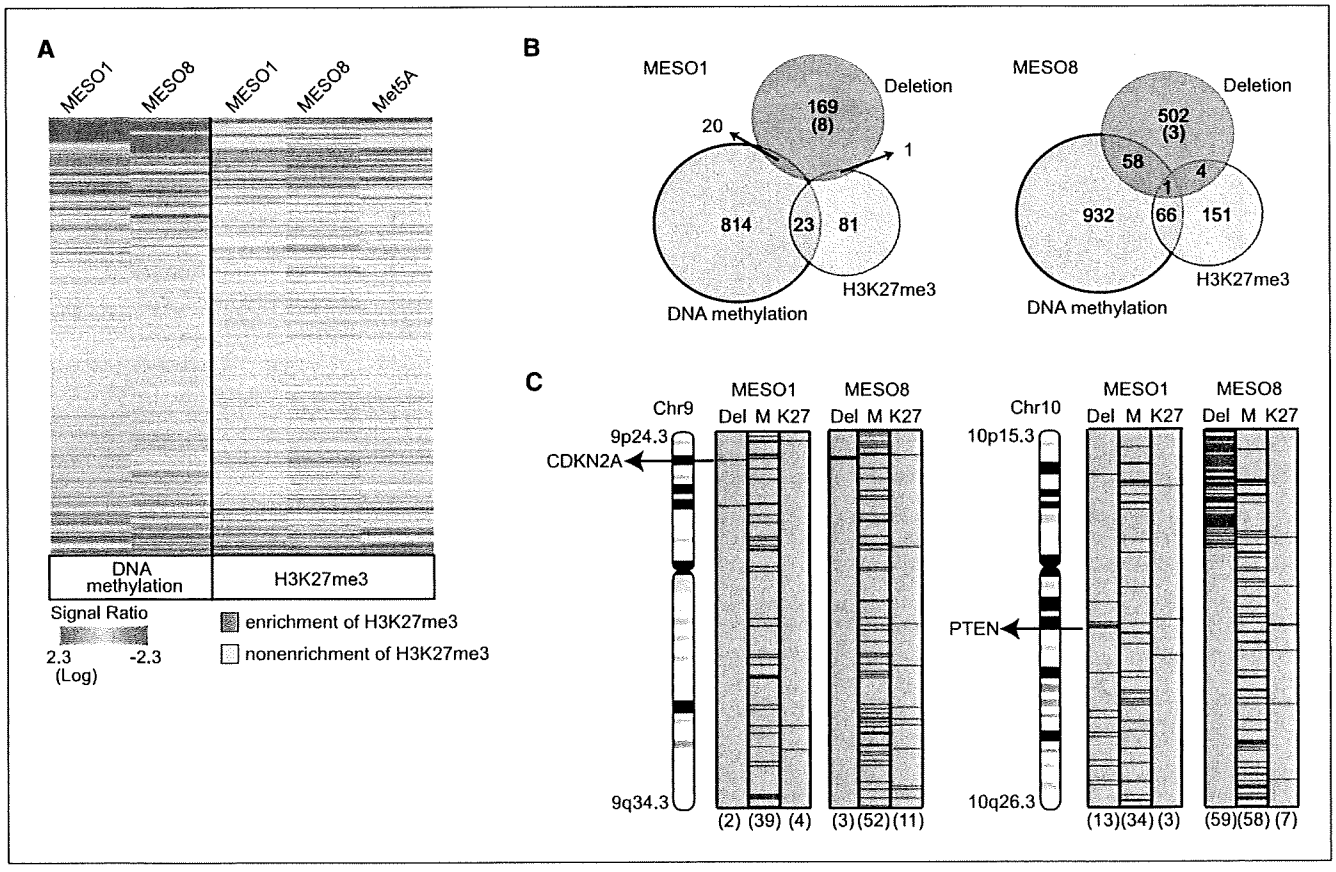

Figure 4. Epigenetic and genetic analysis of MESO1 and MESO8. *A*, unsupervised hierarchical cluster analysis of DNA methylation and H3K27me3 data in two MPM cell lines, MESO1 and MESO8, and a normal mesothelial cell line, MeT-5A, using microarray data of 6,157 genes (*Y axis*). Each cell in the matrix represents the DNA methylation (*red* and *blue*, high and low levels) or H3K27me3 status (*red* and *yellow*, enrichment or nonenrichment of H3K27me3) of each gene in an individual sample. *B*, number of DNA methylation targets, H3K27me3 targets, and deleted genes in MESO1 and MESO8 are shown by Venn diagram. Numbers in parentheses indicate number of homozygously deleted genes. *C*, chromosome view of epigenetic and genetic changes in chromosomes 9 and 10. *Del*, deletion; *M*, DNA methylation; *K27*, H3K27me3. Number of genes involved in each event is shown in parentheses.

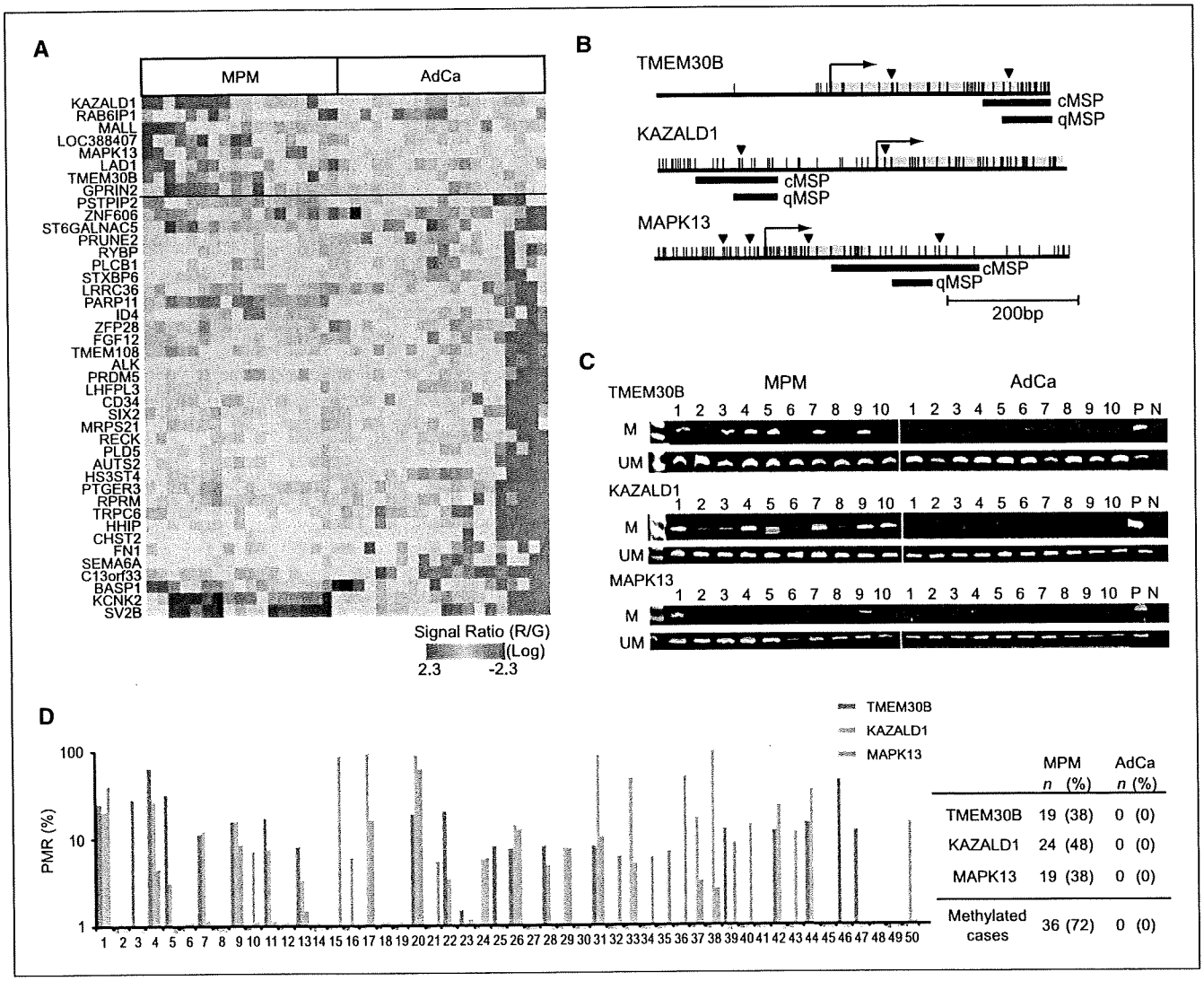

	MPM *n* (%)	AdCa *n* (%)
TMEM30B	19 (38)	0 (0)
KAZALD1	24 (48)	0 (0)
MAPK13	19 (38)	0 (0)
Methylated cases	36 (72)	0 (0)

Figure 5. Identification of specific methylation markers for MPM. *A*, hierarchical clustering using 42 specifically methylated genes in each tumor (8 and 34 genes in MPM and adenocarcinoma, respectively). *B*, diagrams of promoters of three selected genes. Each vertical line represents a single CpG site. The transcription start site (*arrow*), location of exon 1 (*gray box*), *SmaI*/*Xma*I sites (*arrowheads*), and location of MSP assay (*black bar*, *cMSP*, conventional MSP; *qMSP*, quantitative MSP) are indicated. *C*, representative MSP data of *TMEM30B*, *KAZALD1*, and *MAPK13* in the 10 MPM samples and 10 adenocarcinoma samples used for MCAM analysis. DNA methylation was detected in some MPM samples. *M*, methylated form; *UM*, unmethylated form; *P*, positive control; *N*, no DNA template. Positive controls were *Sss*I-treated DNA for the methylated form and DNA from normal lymphocytes for the unmethylated form. *D*, levels of DNA methylation in *TMEM30B* (*blue columns*), *KAZALD1* (*pink columns*), and *MAPK13* (*green columns*) examined by quantitative MSP. *X axis*, MPM cases. Cases 1 to 10 are the same MPM samples as label in *C*. *Y axis*, percentage methylated reference (%). A summary of the quantitative MSP results is given beside the graph. Methylated cases indicate frequency of hypermethylation in at least one of the three genes.

(18, 38). Our results revealed that simultaneous accumulation of DNA methylation was found in adenocarcinoma, which revealed that a subset of adenocarcinoma exhibited CpG island methylator phenotype, whereas MPM rarely did so. Continuous inflammation from asbestos seems to be a driving force in inducing hypermethylation in MPM, and an association between asbestos burden and the methylation profile has been indicated (13, 14). Smoking may act as a stronger epimutagene (39) than asbestos as we have shown here. Nevertheless, these observations might also indicate a distinct mechanism for the acquisition of aberrant DNA methylation during the formation of MPM and adenocarcinoma.

DNA methylation of several genes seems to affect the clinicopathologic phenotype of MPM (40). In this study, we classified MPMs into two groups by methylation profile of a certain gene set; MPMs with low frequency of DNA methylation showed a significantly longer survival rate. These data indicate that accumulation of DNA methylation in multiple loci is one mechanism affecting the progression of this disease.

In the MPM cell lines, we found different responses to epigenetic treatment in silenced genes. A typical DNA methylation target gene, *ANK1*, was reactivated by DNA methyltransferase inhibitor 5Aza-dC but not by HDAC inhibitor trichostatin A alone as reported previously (32). However, two genes, *PENK* and *PGR*, were reactivated by both 5Aza-dC and trichostatin A. Examination of another epigenetic silencing mechanism, H3K27me3, might explain the intricate situation of gene expression in MPMs. When genes are silenced by DNA methylation alone, 5Aza-dC efficiently reactivates the gene; however, trichostatin A is inert in this situation.

When genes are silenced by H3K27me3, both trichostatin A and 5Aza-dC affect gene activity regardless of DNA methylation status. This is consistent with the recent genome-wide analyses of polycomb group–mediated H3K27me3 silencing machinery in prostate cancers showing that a particular set of genes is dominantly silenced by H3K27me3 independent of DNA methylation and can be reactivated by a HDAC inhibitor (21, 41). The reason why silenced *PGR* without DNA methylation was reactivated by 5Aza-dC is not clear (MESO1 in Fig. 3*B*). This might be explained by the several studies suggesting that 5Aza-dC can act independently of its ability to inhibit DNA methylation, inducing the activation of unmethylated genes (42–44).

Integrated analysis of DNA methylation, H3K27me3, and array comparative genomic hybridization data in 5,746 genes in MPM cell lines has revealed that DNA methylation is a major silencing mechanism in CpG promoters and that H3K27me3 regulates a subset of genes, whereas deletions of loci are less frequent. By virtue of this combined analysis, we discovered that, on CpG promoter regions, ~11% of genes were affected by both genetic and epigenetic alterations in MPM, which generally results in their being silenced. These data indicate that multiple epigenetic abnormalities may work in harmony with genetic defects to inactivate a tumor suppressor gene through Knudson's two-hits model, in which a mutation or heterozygous deletion combines with DNA methylation and/or H3K27me3 to inactivate two alleles. Clinical trials using a different HDAC inhibitor, suberoylanilide hydroxamic acid, have been conducted in recurrent MPMs, but that drug is ineffective for the treatment of this disease (45). This might be partially explained by evidence showing that the HDAC inhibitor could not reactivate the genes silenced by DNA methylation. Taken together, our data suggest that the targeting DNA methylation in addition to H3K27me3 might be of great benefit and could improve the treatment of MPM.

DNA methylation has been proposed as a powerful marker for MPM diagnosis (11, 12). However, a previous examination of the methylation status of both MPM and adenocarcinoma showed that hypermethylation of the candidate markers was detected in both MPMs and adenocarcinomas to some extent, although at different frequencies. In addition, methylation markers specific for MPM have not been reported previously. Our analysis showed that hypermethylation of certain loci was frequently detected in MPM and that three genes in particular, *TMEM30B* (46), *KAZALD1* (47), and *MAPK13* (48), were specifically methylated in MPM. Their aberrant methylation could serve as informative markers to distinguish MPMs from adenocarcinomas and could be applicable for the samples obtained from less invasive procedures, such as serum and pleural effusion. A larger study is needed to validate these three genes as useful diagnostic markers for MPM.

In summary, a global methylation analysis comparing MPM and adenocarcinoma can decipher characteristic DNA methylation patterns in MPM. Because multiple epigenetic abnormalities might contribute to tumorigenesis through the silencing of particular cancer-related genes, targeting these epigenetic mechanisms could potentially be effective treatments for clinical use in MPM. Finally, here we propose potential markers that could be of diagnostic value for use in MPMs.

Disclosure of Potential Conflicts of Interest

No potential conflicts of interest were disclosed.

Acknowledgments

Received 4/30/09; revised 8/27/09; accepted 9/15/09; published OnlineFirst 11/3/09.

Grant support: Special Coordination Fund for Promoting Science and Technology from the Ministry of Education, Culture, Sports, Science and Technology of Japan (H18-1-3-3-1; Y. Sekido); Grant-in-Aid for Scientific Research from the Japan Society for the Promotion of Science (Y. Sekido, Y. Kondo); Third-Term Comprehensive Control Research for Cancer and Grant-in-Aid for Cancer Research from the Ministry of Health, Labor, and Welfare (Y. Sekido, Y. Kondo); and 24th General Assembly of the Japanese Association of Medical Sciences (Y. Kondo).

The costs of publication of this article were defrayed in part by the payment of page charges. This article must therefore be hereby marked *advertisement* in accordance with 18 U.S.C. Section 1734 solely to indicate this fact.

We thank Ikuko Tomimatsu and Shoko Mitsumatsu for technical assistance and Shana Straub for critical reading of the article.

MIAME accession numbers: Array Express: E-TABM-813 (MCAM data of 20 MPMs and 20 adenocarcinomas), E-TABM-781 (chromatin immunoprecipitation-microarray in MPM cells), and E-TABM-808 (MCAM data in MPM cells).

References

1. Robinson BW, Lake RA. Advances in malignant mesothelioma. N Engl J Med 2005;353:1591–603.
2. Tsiouris A, Walesby RK. Malignant pleural mesothelioma: current concepts in treatment. Nat Clin Pract Oncol 2007;4:344–52.
3. van Meerbeeck JP, Gaafar R, Manegold C, et al. Randomized phase III study of cisplatin with or without raltitrexed in patients with malignant pleural mesothelioma: an intergroup study of the European Organisation for Research and Treatment of Cancer Lung Cancer Group and the National Cancer Institute of Canada. J Clin Oncol 2005;23:6881–9.
4. Cheng JQ, Jhanwar SC, Klein WM, et al. p16 alterations and deletion mapping of 9p21-22 in malignant mesothelioma. Cancer Res 1994;54:5547–51.
5. Sekido Y, Pass HI, Bader S, et al. Neurofibromatosis type 2 (NF2) gene is somatically mutated in mesothelioma but not in lung cancer. Cancer Res 1995;55:1227–31.
6. Bianchi AB, Mitsunaga SI, Cheng JQ, et al. High frequency of inactivating mutations in the neurofibromatosis type 2 gene (NF2) in primary malignant mesotheliomas. Proc Natl Acad Sci U S A 1995;92:10854–8.
7. Sugarbaker DJ, Richards WG, Gordon GJ, et al. Transcriptome sequencing of malignant pleural mesothelioma tumors. Proc Natl Acad Sci U S A 2008;105:3521–6.
8. Krismann M, Muller KM, Jaworska M, Johnen G. Molecular cytogenetic differences between histological subtypes of malignant mesotheliomas: DNA cytometry and comparative genomic hybridization of 90 cases. J Pathol 2002;197:363–71.
9. Jones PA, Baylin SB. The fundamental role of epigenetic events in cancer. Nat Rev Genet 2002;3:415–28.
10. Perwez Hussain S, Harris CC. Inflammation and cancer: an ancient link with novel potentials. Int J Cancer 2007;121:2373–80.
11. Toyooka S, Pass HI, Shivapurkar N, et al. Aberrant methylation and simian virus 40 tag sequences in malignant mesothelioma. Cancer Res 2001;61:5727–30.
12. Tsou JA, Shen LY, Siegmund KD, et al. Distinct DNA methylation profiles in malignant mesothelioma, lung adenocarcinoma, and non-tumor lung. Lung Cancer 2005;47:193–204.
13. Tsou JA, Galler JS, Wali A, et al. DNA methylation profile of 28 potential marker loci in malignant mesothelioma. Lung Cancer 2007;58:220–30.
14. Christensen BC, Houseman EA, Godleski JJ, et al. Epigenetic profiles distinguish pleural mesothelioma from normal pleura and predict lung asbestos burden and clinical outcome. Cancer Res 2009;69:227–34.
15. Xu L, Flynn BJ, Ungar S, et al. Asbestos induction of extended lifespan in normal human mesothelial cells: interindividual susceptibility and SV40 T antigen. Carcinogenesis 1999;20:773–83.
16. Bocchetta M, Di Resta I, Powers A, et al. Human mesothelial cells are unusually susceptible to simian virus 40-mediated transformation and asbestos cocarcinogenicity. Proc Natl Acad Sci U S A 2000;97:10214–9.
17. Yang H, Bocchetta M, Kroczynska B, et al. TNF-α inhibits asbestos-induced cytotoxicity via a NF-κB-dependent pathway, a possible mechanism for asbestos-induced oncogenesis. Proc Natl Acad Sci U S A 2006;103:10397–402.
18. Toyota M, Ahuja N, Ohe-Toyota M, Herman JG, Baylin SB, Issa JP. CpG island methylator phenotype in colorectal cancer. Proc Natl Acad Sci U S A 1999;96:8681–6.
19. Kirmizis A, Bartley SM, Kuzmichev A, et al. Silencing of human polycomb target genes is associated with methylation of histone H3 Lys 27. Genes Dev 2004;18:1592–605.
20. van der Vlag J, Otte AP. Transcriptional repression mediated by the human polycomb-group protein EED involves histone deacetylation. Nat Genet 1999;23:474–8.
21. Kondo Y, Shen L, Cheng AS, et al. Gene silencing in cancer by histone H3 lysine 27 trimethylation independent of promoter DNA methylation. Nat Genet 2008;40:741–50.

22. Shen L, Kondo Y, Guo Y, et al. Genome-wide profiling of DNA methylation reveals a class of normally methylated CpG island promoters. PLoS Genet 2007;3:2023–36.
23. Gao W, Kondo Y, Shen L, et al. Variable DNA methylation patterns associated with progression of disease in hepatocellular carcinomas. Carcinogenesis 2008;29: 1901–10.
24. Usami N, Fukui T, Kondo M, et al. Establishment and characterization of four malignant pleural mesothelioma cell lines from Japanese patients. Cancer Sci 2006; 97:387–94.
25. Eisen MB, Spellman PT, Brown PO, Botstein D. Cluster analysis and display of genome-wide expression patterns. Proc Natl Acad Sci U S A 1998;95:14863–8.
26. Yang AS, Estecio MR, Doshi K, Kondo Y, Tajara EH, Issa JP. A simple method for estimating global DNA methylation using bisulfite PCR of repetitive DNA elements. Nucleic Acids Res 2004;32:e38.
27. Kondo Y, Shen L, Suzuki S, et al. Alterations of DNA methylation and histone modifications contribute to gene silencing in hepatocellular carcinomas. Hepatol Res 2007;37:974–83.
28. Shen L, Guo Y, Chen X, Ahmed S, Issa JP. Optimizing annealing temperature overcomes bias in bisulfite PCR methylation analysis. Biotechniques 2007;42:48, 50, 2 passim.
29. Eads CA, Lord RV, Wickramasinghe K, et al. Epigenetic patterns in the progression of esophageal adenocarcinoma. Cancer Res 2001;61:3410–8.
30. Kondo Y, Shen L, Issa JP. Critical role of histone methylation in tumor suppressor gene silencing in colorectal cancer. Mol Cell Biol 2003;23:206–15.
31. Ogino S, Cantor M, Kawasaki T, et al. CpG island methylator phenotype (CIMP) of colorectal cancer is best characterised by quantitative DNA methylation analysis and prospective cohort studies. Gut 2006;55: 1000–6.
32. Cameron EE, Bachman KE, Myohanen S, Herman JG, Baylin SB. Synergy of demethylation and histone deacetylase inhibition in the re-expression of genes silenced in cancer. Nat Genet 1999;21:103–7.
33. Taniguchi T, Karnan S, Fukui T, et al. Genomic profiling of malignant pleural mesothelioma with array-based comparative genomic hybridization shows frequent non-random chromosomal alteration regions including JUN amplification on 1p32. Cancer Sci 2007; 98:438–46.
34. Flotho C, Paulun A, Batz C, Niemeyer CM. AKAP12, a gene with tumour suppressor properties, is a target of promoter DNA methylation in childhood myeloid malignancies. Br J Haematol 2007;138:644–50.
35. Belinsky SA. Gene-promoter hypermethylation as a biomarker in lung cancer. Nat Rev Cancer 2004;4:707–17.
36. Estecio MR, Yan PS, Ibrahim AE, et al. High-throughput methylation profiling by MCA coupled to CpG island microarray. Genome Res 2007;17:1529–36.
37. Weber M, Hellmann I, Stadler MB, et al. Distribution, silencing potential and evolutionary impact of promoter DNA methylation in the human genome. Nat Genet 2007;39:457–66.
38. Suzuki M, Shigematsu H, Iizasa T, et al. Exclusive mutation in epidermal growth factor receptor gene, HER-2, and KRAS, synchronous methylation of non-small cell lung cancer. Cancer 2006;106:2200–7.
39. Grady WM. CIMP and colon cancer gets more complicated. Gut 2007;56:1498–500.
40. Fischer JR, Ohnmacht U, Rieger N, et al. Promoter methylation of RASSF1A, RARβ and DAPK predict poor prognosis of patients with malignant mesothelioma. Lung Cancer 2006;54:109–16.
41. Gal-Yam EN, Egger G, Iniguez L, et al. Frequent switching of Polycomb repressive marks and DNA hypermethylation in the PC3 prostate cancer cell line. Proc Natl Acad Sci U S A 2008;105:12979–84.
42. Milutinovic S, Knox JD, Szyf M. DNA methyltransferase inhibition induces the transcription of the tumor suppressor p21(WAF1/CIP1/sdi1). J Biol Chem 2000; 275:6353–9.
43. Soengas MS, Capodieci P, Polsky D, et al. Inactivation of the apoptosis effector Apaf-1 in malignant melanoma. Nature 2001;409:207–11.
44. Wozniak RJ, Klimecki WT, Lau SS, Feinstein Y, Futscher BW. 5-Aza-2′-deoxycytidine-mediated reductions in G9A histone methyltransferase and histone H3 K9 di-methylation levels are linked to tumor suppressor gene reactivation. Oncogene 2007;26:77–90.
45. Ramalingam SS, Belani CP, Ruel C, et al. Phase II study of belinostat (PXD101), a histone deacetylase inhibitor, for second line therapy of advanced malignant pleural mesothelioma. J Thorac Oncol 2009;4: 97–101.
46. Furuta J, Nobeyama Y, Umebayashi Y, Otsuka F, Kikuchi K, Ushijima T. Silencing of peroxiredoxin 2 and aberrant methylation of 33 CpG islands in putative promoter regions in human malignant melanomas. Cancer Res 2006;66:6080–6.
47. Shibata Y, Tsukazaki T, Hirata K, Xin C, Yamaguchi A. Role of a new member of IGFBP superfamily, IGFBP-rP10, in proliferation and differentiation of osteoblastic cells. Biochem Biophys Res Commun 2004;325: 1194–200.
48. Ehrlich M, Sanchez C, Shao C, et al. ICF, an immunodeficiency syndrome: DNA methyltransferase 3B involvement, chromosome anomalies, and gene dysregulation. Autoimmunity 2008;41:253–71.

EXPERT REVIEWS

Gefitinib for the treatment of non-small-cell lung cancer

Expert Rev. Anticancer Ther. 9(1), 17–35 (2009)

Toyoaki Hida†,
Shizu Ogawa,
Jang Chul Park,
Ji Young Park,
Junichi Shimizu,
Yoshitsugu Horio and
Kimihide Yoshida
†*Author for correspondence*
Department of Thoracic Oncology, Aichi Cancer Center Hospital, 1-1 Kanokoden, Chikusa-ku, Nagoya 464-8681, Japan
Tel.: +81 527 626 111
Fax: +81 527 642 963
107974@aichi-cc.jp

Gefitinib is an orally bioavailable, EGF receptor tyrosine kinase inhibitor and was the first targeted drug to be approved for non-small-cell lung cancer (NSCLC). Identification of objective tumor regressions with gefitinib in NSCLC patients has resulted in intense, worldwide clinical and basic research directed toward finding the optimal use of gefitinib in NSCLC. A recent large international Phase III study (IRESSA NSCLC Trial Evaluating Response and Survival Against Taxotere [INTEREST]) comparing gefitinib and docetaxel in unselected pretreated patients showed equivalent survival with better tolerability and quality of life. In addition, a Phase III study (WJTOG0203) evaluating gefitinib as sequential therapy after platinum-doublet chemotherapy showed the improved progression-free survival time. Furthermore, a large-scale randomized study (IRESSA Pan-Asia study [IPASS]) comparing gefitinib monotherapy with carboplatin/paclitaxel for previously untreated patients with adenocarcinoma who were never- or light-smokers showed an improved progression-free survival time in the gefitinib arm. A smaller Phase III study of pretreated Japanese patients (V-15-32) also demonstrated no difference in overall survival compared with docetaxel, with a statistically greater overall response rate. Somatic mutations in the *EGFR* gene, the target of gefitinib, were associated with dramatic and durable regressions in patients with NSCLC. Currently, investigators are trying to determine the optimal approach to select patients for treatment with gefitinib. This article aims to briefly summarize the profile of gefitinib, *EGFR* mutations, landmark trials with gefitinib and, also, ongoing trials that may herald an era of individualized therapy in at least some NSCLC patients.

KEYWORDS: EGF receptor • *EGFR* gene mutation • gefitinib • non-small-cell lung cancer • tyrosine kinase inhibitor

Lung cancer is the most common cause of cancer deaths worldwide. Lung cancer is divided into two morphological types: small-cell lung cancer (SCLC) and non-small-cell lung cancer (NSCLC). SCLC is a distinct clinicopathological entity with a highly aggressive clinical course and neuroendocrine properties. Patients with SCLC are generally more sensitive to a variety of cytotoxic drugs and radiation therapy compared with NSCLC patients. NSCLC, which is less sensitive to chemotherapeutic agents, accounts for over 80% of all lung cancers and NSCLC can be further subdivided by histological type into adenocarcinoma, squamous-cell carcinoma, large-cell carcinoma and others. Adenocarcinoma is the predominant histological subtype and is increasing among patients with lung cancer. Among adenocarcinoma bronchioloalveolar carcinoma is a well-differentiated subtype originating in the peripheral lung that spreads through the airways.

Currently, platinum-based combination chemotherapy regimens, including several active new chemotherapeutic agents, comprise the standard option for patients with advanced NSCLC and good performance status. However, various combinations of drugs have similar efficacy, producing objective response rates of 30–40%, a median survival time of 8–10 months and 1-year survival rates of 30–40% [1–3]. These results remain unsatisfactory and new modalities of treatment are urgently awaited. Recently, novel molecular-targeted strategies that block cancer progression pathways have been suggested as a more cancer cell-specific treatment to control cancer and are considered an exciting therapeutic approach for treating NSCLC [4]. The development of agents that target the EGF receptor (EGFR) signal transduction pathways have provided a class of novel targeted therapeutic agents with improved side-effect profiles compared with conventional chemotherapeutic agents. EGFR is a promising target for anticancer therapy because it is expressed in a variety of tumors, including NSCLC [5]. Furthermore, high levels of EGFR expression have been associated with a poor prognosis in lung cancer patients in several studies.

 10.1586/14737140.9.1.17 ISSN 1473-7140

EGFR-targeted cancer therapies are being developed currently, and gefitinib (IRESSA®; AstraZeneca, Wilmington, DE, USA) is an orally active, selective EGFR tyrosine kinase inhibitor (TKI) that blocks signal transduction pathways implicated in the proliferation and survival of cancer cells.

Overview of the market

Lung cancer frequently presents at an advanced and biologically aggressive stage, resulting in poor prognosis. Surgery, chemotherapy and radiation have been generally unsatisfactory, especially in the treatment of advanced disease, and new strategies based on better understanding of the biology are clearly needed to improve the treatment efficacy of this fatal disease. The development of agents that target EGFR signal transduction pathways have provided a class of novel targeted therapeutic agents. Different approaches to inhibiting EGFR have resulted in a number of EGFR-targeted agents in clinical development, including small-molecule EGFR TKIs and monoclonal antibodies. The role of cetuximab (Erbitux®), a monoclonal antibody directed at the extracellular domain of the EGFR, and of gefitinib and erlotinib (Tarceva®; OSI Pharmaceuticals, NY, USA), oral, low-molecular-weight ATP-competitive inhibitors of the EGFR's tyrosine kinase domain is under investigation. Anti-EGFR monoclonal antibodies have demonstrated activity in the therapy of advanced colorectal carcinoma [6] and in a variety of epithelial tumor types, including head and neck cancer and NSCLC. A large Phase III study has found that targeted therapy with cetuximab, combined with platinum-based chemotherapy, improves survival outcome as a first-line treatment for patients with advanced NSCLC (overall survival [OS]: 11.3 months vs 10.1 months; $p = 0.044$) [7]. Erlotinib is another TKI with slightly different pharmacologic characteristics from gefitinib. Similar to gefitinib, erlotinib is a potent inhibitor of EGFR autophosphorylation, with a concentration that inhibits 50% in the nanomolar range *in vitro*. Erlotinib is the only EGFR TKI approved based on demonstrating improved survival versus placebo, which was observed in patients with advanced NSCLC who had been treated previously with chemotherapy. The randomized study (BR.21 study) brought erlotinib to registration by the US FDA on November 19, 2004, for the treatment of second- and third-line advanced NSCLC [8]. Other EGFR TKIs are currently under investigation in Phase I/II trials, many of which have differing selectivities for the various members of the human EGFR family. In the near future, gefitinib and erlotinib may face competition from EGFR-specific TKIs, such as EKB-569 (Wyeth, Maidenhead, UK) and CL-387785 (Calbiochem, CA, USA), and EGFR-family TKIs, such as BIBW-2992 (Boehringer Ingelheim, Berkshire, UK), HKI-272 (Wyeth), PKI-166 (Novartis), GW-572016 (GlaxoSmithKline, NC, USA), CI-1033 (Pfizer, MI, USA) and PF-00299804 (Pfizer). The VEGF pathway forms another target for cancer treatment, because the growth of solid tumor is angiogenesis dependent. VEGF and EGF exert their biological effects directly or indirectly on tumor growth and metastasis/invasion, as well as on tumor angiogenesis. The biological effects by VEGF and EGF are mediated through activation of their specific downstream signaling, but both factors also share common downstream signaling pathways. There is, thus, the potential for improved therapeutic efficacy by the combination of both EGF/EGFR-targeting and VEGF/VEGF receptor-targeting drugs, although they have a different side-effect profile. It may also face competition later on from multitargeted TKIs, such as ZD6474 (AstraZeneca), AEE-788 (Novartis) and XL647 (Exelixis Inc., San Francisco, CA, USA). Karaman *et al.* have reported small-molecule kinase interaction maps, which provide a useful graphic overview of how compounds interact with the kinome [9].

Gefitinib: an EGFR TKI

Gefitinib is the first molecularly targeted agent to be registered for advanced NSCLC. In Phase II clinical trials, the selective and orally active EGFR TKI gefitinib produced objective tumor responses and symptom improvement in patients with NSCLC who had previously received chemotherapy (response rates of 12–18% and symptom improvement rates of 40–44% in IRESSA Dose Evaluation in Advanced Lung Cancer [IDEAL]-1 and -2) [10,11]. Partial clinical responses to gefitinib have been observed most frequently in women, never-smokers and patients with adenocarcinomas. The IRESSA Survival Evaluation in Lung Cancer (ISEL) study also showed a survival benefit for gefitinib over placebo in Asian patients and never-smokers [12]. Thus, gefitinib clinical trials have shown that higher response rates and longer survival are associated with specific patient characteristics. Using conventional doublet chemotherapy simultaneously with gefitinib or erlotinib in unselected first-line patients does not increase survival [13–16], but the results of a recent Phase III study showed that gefitinib improves progression-free survival (PFS) as sequential therapy after platinum-doublet chemotherapy [17]. The Phase III IRESSA NSCLC Trial Evaluating Response and Survival Against Taxotere (INTEREST) and V-15-32 studies comparing gefitinib and docetaxel in unselected pretreated patients showed no difference in OS, suggesting that gefitinib and docetaxel were equally effective as the second-line therapy [18,19]. In addition, the Phase III IRESSA Pan-Asia study (IPASS) comparing gefitinib monotherapy with carboplatin/paclitaxel showed an improved PFS time in the gefitinib arm [20]. On the other hand, molecular studies have revealed that EGFR-activating mutations and high *EGFR* gene copy number are frequently found in patients who have the best outcomes with EGFR TKIs [21–27]. Currently, investigators are trying to determine the optimal approach to selecting patients for treatment with EGFR TKIs. Gefitinib is the first class of oral targeted therapies to produce such responses in advanced NSCLC and the most studied agent in clinical trials.

Chemistry

Gefitinib, 4-(3-chloro-4-fluoroanilino)-7-methoxy-6-(3-morpholinopropoxy) quinazoline (ZD1839, IRESSA; Figure 1), is an orally active, low-molecular-weight (447 kDa) quinazolin derivative

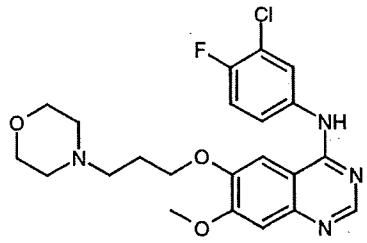

Figure 1. Gefitinib.

with a molecular formula $C_{22}H_{24}ClFN_4O_3$ that specifically inhibits the activation of EGFR tyrosine kinase through competitive binding of the ATP-binding domain of the receptor.

It is readily soluble at pH1 and highly insoluble above pH7. Gefitinib is very stable at room temperature with a proven shelf-life of 36 months [28].

Pharmacodynamics

Gefitinib selectively inhibits the activation of EGFR tyrosine kinase through competitive binding of the ATP-binding domain of the receptor. Selectivity was demonstrated versus HER2 and the VEGF tyrosine kinases, kinase insert domain receptor and Flt-1, with at least a 100-fold difference in IC_{50} for EGFR compared with other tyrosine kinases. Similarly, gefitinib did not inhibit the activity of the serine threonine kinases raf, MEK-1 and ERK-2 (MAPK) [29]. In the Phase I trials, the maximum tolerated dosage was 700 mg/day, although dosages as low as 150 mg/day provided plasma concentrations sufficient for pharmacological activity, evidence of targeted biological effect and anti-tumor activity [30–33]. An analysis of pharmacodynamics marker levels in the skin also provided evidence that sufficient gefitinib was reaching the skin and inhibiting EGFR signaling at 150 mg/day [34]. Additionally, objective tumor responses observed across a dosage range of 150–1000 mg/day indicated that these dosages resulted in target inhibition in tumors. Two large Phase II trials (IDEAL-1 and -2) evaluated 250- and 500-mg/day dosages of gefitinib in patients with advanced NSCLC. As predicted from the Phase I trials, dosages of more than 250 mg/day provided no additional efficacy benefit, whereas adverse effects increased in a dose-dependent manner. Consequently, the recommended dose of gefitinib in NSCLC is 250 mg/day [10,11]. Pharmacodynamic studies indicate that gefitinib blocks cell cycle progression in the G_1 phase by upregulating $p27^{Kip1}$, a cell cycle inhibitor, and downregulating c-fos, a transcriptional activator that is prominent in EGFR-mediated signaling [35]. Elevated levels of $p27^{Kip1}$ block cell cycle progression in the G_1 phase of growth. This sustains the hypophosphorylated state of the *Rb* gene product, which is necessary to keep cells from progressing in the cell cycle [36]. The inhibition of tumor growth seen with gefitinib is also accompanied by decreases in VEGF, basic FGF and TGF-α, all potent inducers of tumor angiogenesis [37]. Thus, gefitinib may also inhibit tumor growth by interfering with angiogenesis. These observations suggest that by inhibiting the EGFR tyrosine kinase, gefitinib treatment alters expression levels of key molecules in tumor cells that are important for stimulating proliferation, cell cycle progression, tumor angiogenesis, metastasis and inhibition of apoptosis. Gefitinib treatment can also cause apoptosis to occur *in vitro*, the frequency of which correlates with the cell line sensitivity to the drug and provides a link with the tumor shrinkage reported clinically [38].

Pharmacokinetics & metabolism

The pharmacokinetic profile revealed that gefitinib is orally bioavailable and suitable for once-daily dosing in cancer patients. In healthy volunteer studies, gefitinib was absorbed moderately slowly, reaching C_{max} 3–7 h after administration. The elimination half-life of 28 h suggests that once-daily oral administration is appropriate [34]. In the initial Phase I studies of gefitinib, sequential skin biopsies were performed prior to and after 4 weeks of therapy [34]. The skin was selected as the target tissue due to its easy access and the established role of the EGFR in renewal of the dermis. Inhibition of EGFR phosphorylation and EGFR-dependent downstream processes was detected at dosages of 150 mg/day, well below the maximal tolerable dosage (MTD) of 700 mg/day. In a clinical study (BCIRG 103), gefitinib (250 mg) was administered orally to breast cancer patients for at least 14 days [39]. Gefitinib concentrations in each tumor sample (mean: 7.5 μg/g) were substantially higher (mean: 42-fold) than the corresponding plasma sample (mean: 0.18 μg/ml). Haura *et al.* conducted a pilot Phase II study of a 28-day preoperative course of gefitinib 250 mg orally, followed by surgical resection for patients with stage IA to selected IIIA NSCLC [40]. Tumor penetration of gefitinib was assessed in surgically resected tumor samples along with plasma assessment on day 28. Day 28 plasma concentrations of gefitinib averaged 531 ± 344 nM (range: 65–1211 nM) while tumor concentrations of gefitinib averaged 33,108 ± 44,312 nM (range: 74–134,669 nM). These results also demonstrate that NSCLC tumor penetration of gefitinib is high, as its tumor concentrations were much higher than concentrations found in plasma.

Gefitinib is metabolized extensively by expressed cytochrome P450 (CYP)3A4, producing a similar range of metabolites to liver microsomes, while CYP3A5 produced a range of metabolites, similar to CYP3A4 but to a much lower degree [41,42]. By contrast, CYP2D6 catalyzed rapid and extensive metabolism of gefitinib to desmethyl-gefitinib (M523595). While formation of M523595 was CYP2D6 mediated, the overall metabolism of gefitinib was dependent primarily on CYP3A4. Quantitatively, the most important routes of gefitinib metabolism were mediated primarily by CYP3A4, while CYP3A5 and CYP2D6 were minor contributors. The wide variability in CYP3A4 activity in human liver is probably a significant factor in the interindividual variability observed in gefitinib pharmacokinetics. Gefitinib has interactions with CYP3A4 inducers, or CYP3A4 enzyme inhibitors or substrate of CYP2D6 (gefitinib inhibits CYP2D6 activity) or H2 blockers. Pharmacokinetic studies have shown that the bioavailability of gefitinib is unaffected by food intake to any clinically significant extent [43].

Clinical efficacy

Several challenges were encountered in designing the clinical trials of gefitinib, because this agent was expected to be cytostatic rather than cytotoxic. These challenges included a scarcity of precedents, the way in which 'biological activity' was defined, the integration of outcomes across multiple tumor types in Phase I trials, the relationship between biological activity and clinical outcome, and unknown pharamakokinetic and pharmacodynamic relationships. Initially, clinical trials of gefitinib were performed principally in unselected patient populations with NSCLC. However, recent results indicate that different patients derive different degrees of clinical benefit from treatment with gefitinib. The identification of the patients who are most likely to derive clinical benefit from gefitinib is of paramount importance.

Phase I

As biologically targeted agents are expected to provide clinical benefits that are not predicted by surrogate end points of toxicity to normal replicating tissue, new Phase I trials have been designed to determine the optimum biological dose for use in further studies. Initial Phase I trials performed in healthy volunteers showed that oral administration of gefitinib given once on day 1 (50, 100, 250 or 500 mg) or daily for 14 days (100 mg/day) was feasible [44]. Four multicenter Phase I trials then evaluated the safety profile of gefitinib (50–1000 mg/day) in more than 250 patients with a wide range of solid tumors that were known to express EGFR, although baseline EGFR expression levels were not determined [30–32,45]. Adverse events (AEs) occurred at dosages of 50 mg/day, with the most commonly reported AEs being mild-to-moderate acne-like rash, diarrhea, nausea, anorexia, vomiting and asthenia. The frequency of AEs, such as skin rash and diarrhea, increased with dose, and the MTD was identified as 700 mg/day. Clinical benefit was not dose-related, whereas the most common AEs (skin rash and acne) increased with gefitinib dose. In addition, pharmacokinetic studies indicated that plasma levels of gefitinib over this dose range were sufficient for effective EGFR inhibition. Although the lowest dose at which objective tumor responses were observed was 150 mg/day, there was potential for individuals receiving this dose to have subtherapeutic exposure as a result of interpatient variability in pharmacokinetics. Accordingly, the slightly higher dosage of 250 mg/day was chosen. The second dosage chosen was 500 mg/day, which was the highest dosage that was well tolerated by most patients on a daily dosing schedule. Both dosages were significantly lower than the MTD, unlike conventional dosage selection for chemotherapy agents, which would use the MTD.

Phase II

Large-scale dose-evaluation study

Two large, dose-randomized, double-blind, parallel-group, multicenter Phase II trials (IDEAL-1 and -2) independently evaluated the activity of gefitinib 250 and 500 mg/day in 425 patients with advanced NSCLC [10,11]. These trials allowed a more detailed evaluation of the doses selected from the Phase I trials and included symptom improvement as an additional end point. In IDEAL-1, conducted mainly in Europe and Japan, patients with one or two prior chemotherapy regimens, including a platinum compound, were randomly assigned to receive gefitinib at 250 or 500 mg/day. Response rate approached 20% and was similar in both arms, and symptom improvement was 40%, which was higher in patients who had an objective response. Adverse effects were, in general, well tolerated, but were more severe with the 500-mg dose. In IDEAL-2, the study was performed in 30 centers in the USA. In total, 221 patients were randomly assigned to receive either gefitinib 250 or 500 mg daily. A total of 126 patients (58%) had three or more regimens in the past and 65% had histology of adenocarcinoma. Symptoms of NSCLC improved in 43% of patients receiving gefitinib 250 mg and in 35% of those receiving 500 mg. There was no significant difference in response rate or survival between the two doses. There was a good correlation between clinical response and symptomatic improvement. However, the gefitinib 500-mg dose was more toxic as it induced more acne-like rash and diarrhea. In conclusion, gefitinib was well tolerated at 250 mg/day and it induced anti-tumor activity in approximately 10% of patients. These results are impressive compared with chemotherapy, which induces far more adverse effects and, probably, even a lower level of activity.

Gefitinib as first-line treatment

In East Asia, Phase II trials of gefitinib as first-line therapy have demonstrated good response rates of 30% compared with those in patients of non-East Asian origin (<10%) [46–51]. In a prospective Phase II trial of chemotherapy-naive patients with advanced NSCLC conducted in Japan, 40 patients treated with first-line gefitinib were evaluated for response. Partial response was seen in 12 (30%) patients [47]. Response to gefitinib in studies of non-Asian patients have been shown to be much lower than in studies of Asian patients. In a study in the USA, response rate among 70 patients with advanced NSCLC and poor performance status (2 or 3) was 4% [50]. In Germany, response rate among 58 patients with inoperable advanced NSCLC and good performance status (0–2) was 5% [49]. Results from IRESSA in NSCLC versus Vinorelbine Investigation in the Elderly (INVITE) reported no statistical difference between gefitinib and chemotherapy first-line for median PFS rates (2.7 vs 2.9 months, respectively) or overall response rates (3.1 vs 5.1%, respectively) [52,53]. Iressa NSCLC Trial Evaluating Poor Performance Patients (INSTEP) reported a response rate of 6% and a trend toward improved efficacy end points with gefitinib first-line compared with placebo, with similar improvements in quality of life and symptoms in Western patients with poor performance status [54]. See Table 1 for a detailed list.

Gefitinib therapy in selected patients

Table 2 lists several reports on gefitinib sensitivity in selected patients [55–66]. In 2004, several investigators reported that somatic mutations in the gene for the EGFR [21–23], the targets

Table 1. Phase II studies of gefitinib.

Author/study	Treatment arms	Number	ORR (%)	PFS (months)	MST (months)	Comments	Ref
Gefitinib in the second- and third-line treatment of advanced NSCLC							
Fukuoka *et al.* (IDEAL-1)	Gefitinib 250 mg daily	103	18.4	2.7	7.6*	Randomized Phase II trial conducted mainly in Europe and Japan	[10]
	Gefitinib 500 mg daily	105	19.0	2.8	8.0		
Kris *et al.* (IDEAL-2)	Gefitinib 250 mg daily	102	12.0	NA	7.0**	Randomized Phase II trial conducted in the USA	[11]
	Gefitinib 500 mg daily	114	9.0		6.0		
Gefitinib in the first-line treatment of patients with NSCLC							
Goss *et al.* (INSTEP)	Gefitinib	100	6.0			Randomized Phase II trial in patients with poor performance status; modest benefit seen with gefitinib	[54]
	Placebo	101	1.0				
Crino *et al.* (INVITE)	Gefitinib	97	3.1	2.7		Randomized Phase II trial in elderly patients; similar efficacy observed	[52]
	Vinorelbine	99	5.1	2.9			
Niho *et al.*	Gefitinib 250 mg	40	30.0	NA	13.9		[47]
Lin *et al.*	Gefitinib 250 mg	53	32.1	3.2	9.4		[46]
Suzuki *et al.*	Gefitinib 250 mg	34	26.5		14.1		[48]
Reck *et al.*	Gefitinib 250 mg	58	5.0	1.6	6.7		[49]
Spigel *et al.*	Gefitinib 250 mg	70	4.0	3.7	6.3	Patients with poor performance status	[50]
Swinson *et al.*	Gefitinib 250 mg	41	10.0	1	2.7	Patients unsuitable for chemotherapy	[51]
Gefitinib compared with docetaxel in third-line treatment of NSCLC							
Cufer *et al.* (SIGN)	Gefitinib 250 mg	68	13.2	3.0	7.5***	Open label,randomized Phase II study; fewer drug-related side effects with gefitinib	[114]
	Docetaxel 75 mg/m^2	73	13.7	3.4	7.1		

*p = NS.
**p = 0.40.
***p = 0.88.
HR: Hazard ratio; IDEAL: IRESSA Dose Evaluation in Advanced Lung Cancer; INVITE: Iressa in NSCLC versus Vinorelbine Investigation in the Elderly; MST: Median survival time; NA: Not available; NS: Not significant; NSCLC: Non-small-cell lung cancer; ORR: Overall response rate; PFS: Progression-free survival.

of gefitinib, were associated with dramatic and durable regressions with gefitinib in patients with NSCLC. To confirm the encouraging but retrospective results of early studies, multiple groups undertook prospective Phase II trials of gefitinib in patients found to have an *EGFR* mutation on screening. To date, at least nine studies have been reported [55–63]. Collectively, these showed that nearly 80% of patients whose tumors had either exon 19 deletions or L858R mutations had radiographic responses to gefitinib, although responses varied between different trials. The combined analysis of seven prospective trials conducted in Japan, which examined the efficacy and safety of gefitinib monotherapy for NSCLC with *EGFR* mutations, has been reported. In this study, Morita *et al.* updated OS and PFS data for the combined survival analysis and examined prognostic factors for OS and PFS (l-CAMP study) [67]. A total of 148 patients were combined from the seven trials and median OS and PFS of 24.3 months and 9.7 months weer reported, respectively. The combined response rate was 76.4%, and only 6% of the patients had progressive disease. They concluded that gefitinib produces significant anti-tumor activity and prolonged survival in this selected NSCLC population. A prospective Phase II study has also demonstrated that gene copy number assessed by fluorescent *in situ* hybridization (FISH) [25] may predict clinical outcome in TKI-treated NSCLC patients. In advanced bronchioloalveolar carcinoma, a distinct subtype of adenocarcinoma, gefitinib was clinically active in both chemotherapy-naive and pretreated patients [65,66].

Phase III

Gefitinib in combination with chemotherapy

The IRESSA NSCLC Trial Assessing Combination Treatment (INTACT)-1 and -2 studies were large randomized studies of two dosages of gefitinib (250 or 500 mg/day), or placebo, in combination with two different chemotherapy regimens [13,14]. INTACT-1 used cisplatin and gemcitabine (cisplatin 80 mg/m^2 on day 1 and gemcitabine 1250 mg/m^2 on days 1 and 8 every

Table 2. Phase II studies of gefitinib in selected patients.

Author	Selection	Patients (n)	Response rate (%)	TTP/PFS (months)	MST (months)	1-year survival (%)	Ref.
EGFR selected							
Inoue *et al.*	Mutation	16	75	9.7	NR	NR	[55]
Sutani *et al.*	Mutation	27	78	9.4	15.4	NR	[56]
Asahina *et al.*	Mutation	16	75	8.9	NR	88	[57]
Sunaga *et al.*	Mutation	19	84	13	NR	NR	[58]
Yoshida *et al.*	Mutation	21	90	7.7	NR	NR	[59]
Tamura *et al.*	Mutation	28	75	11.5	NR	79	[60]
Sugio *et al.*	Mutation	16	50	8.8	15.4	NR	[61]
Sequist *et al.* (iTARGET)	Mutation*	31	55	9.2	17.5	73	[62]
Yang *et al.*	Mutation‡	43	84	8.9	24		[63]
	Mutation§	12	16	2.1	6.7		
Cappuzzo *et al.* (ONCOBELL)	FISH	42	48	6.4	NR	64	[25]
Never-smokers							
Lee *et al.*		72	55	5.5	19.7	76	[64]
Cappuzzo *et al.*	Never smoker or FISH)	42	48	6.4	NR	64	[25]
Bronchioloalveolar carcinoma							
West *et al.*		101	17	4	13	51	[65]
Cadranel *et al.*		88	13	2.9	13.3	55	[66]

*EGFR mutations were primarily exon 19 deletions (53%) and L858R (26%), although 21% of mutation-positive cases had less-common subtypes, including exon 20 insertions, T790M/L858R, G719A and L861Q.
‡Del 19 or L858R.
§Other mutations.
EGFR: EGF receptor; MST: Median survival time; NR: Not reported; PFS: Progression-free survival time; TTP: Time to progression.

3 weeks), whereas INTACT-2 used carboplatin and paclitaxel (carboplatin given at AUC of 6 and paclitaxel at 225 mg/m^2 in 3-h infusions every 3 weeks). Chemotherapy was administered for up to six cycles and gefitinib or placebo were continued in nonprogressing patients until progression. A total of 1093 and 1037 patients were entered, respectively, in the two studies in less than 1 year of accrual. These two large randomized studies failed to demonstrate a survival increase with the addition of gefitinib to standard chemotherapy in first-line treatment of advanced NSCLC. A subset analysis of patients with adenocarcinoma who received 90 days of chemotherapy or more in the INTACT-2 study demonstrated statistically significant prolonged survival, suggesting a gefitinib maintenance effect. In general, treatment was well tolerated and the toxicity of chemotherapy did not overlap with gefitinib treatment, which made the studies feasible. However, as expected, gefitinib 500 mg was associated with a higher degree of toxicity, as observed in the IDEAL studies, which led to more dose reductions and treatment interruptions. In none of these studies were patients selected based on EGFR expression or any other marker of efficacy, and this lack of patient selection may have caused the lack of positive outcome. In addition, the antagonistic effect of EGFR TKIs may also halt cells in the G_1 phase of their cycle and, therefore, render them insensitive to chemotherapy. Interestingly, however, the time-to-progression curves and survival curves suggest that maintenance EGFR inhibition may be helpful after termination of chemotherapy. These considerations would suggest that sequential therapies are the best approach to this disease for front-line therapy.

The Southwest Oncology Group trial, SWOG0023, was designed to deliver gefitinib after completion of chemoradiotherapy and consolidation chemotherapy, avoiding a potentially negative interaction with chemotherapy. In this randomized, placebo-controlled trial in unresectable stage III NSCLC, gefitinib maintenance therapy failed to show a survival advantage in an unplanned interim analysis; the inferior survival observed in the gefitinib arm raises the possibility of a deleterious effect [68]. The reasons for this result remain unclear. Recently,

Hida *et al.* reported the results of a randomized Phase III trial (WJTOG0203), which evaluated whether gefitinib improves survival as sequential therapy after platinum-doublet chemotherapy in advanced NSCLC (stage IIIb/IV) [17]. In this study, sequential gefitinib following dual platinum-based induction therapy improved PFS (hazard ratio [HR]: 0.68; 95% confidence interval [CI]: 0.57–0.80; $p < 0.001$), with a trend toward improved overall survival ($p = 0.10$). Furthermore, a prespecified subset analysis showed that gefitinib significantly increased overall survival for patients with adenocarcinoma (n = 467; HR: 0.79; 95% CI: 0.65–0.98; $p = 0.03$) and for smokers (n = 410; HR: 0.79; 95% CI: 0.64–0.98; $p = 0.03$). However, gefitinib failed to show a significant survival advantage in patients with nonadenocarcinoma. These results demonstrate a possible clinical benefit for sequential therapy of gefitinib, especially in adenocarcinoma histology. Regarding the maintenance effects, although no benefit with concurrent EGFR TKI was seen in response rate, PFS or OS in the INTACT 2 and Tarceva responses in conjunction with paclitaxel and carboplatin (TRIBUTE) trials, landmark analyses of them favored patients receiving single-agent TKI maintenance therapy after completion of chemotherapy (Table 3) [14,15].

Gefitinib versus best supportive care

In the ISEL study, 1692 patients from 28 countries (not including Japan) were randomized to receive gefitinib 250 mg/day versus placebo [12]. Approximately 20% of the patients included in the study were Asians. Among the subjects, 1129 were assigned to the gefitinib group and 563 to the placebo group. Although the response rate was similar to that observed with erlotinib in BR.21 [8], in the ISEL study, gefitinib failed to prolong survival in comparison with placebo in the overall population. As for the differences in the ISEL and BR.21 patient populations, 90% of the patients in ISEL were chemorefractory, while patients in BR.21 were not required to be refractory to their previous treatment [8,12]. Median survival was 5.6 months for gefitinib and 5.1 months for placebo ($p = 0.08$; HR: 0.89; 95% CI: 0.77–1.02). Among the 812 patients with adenocarcinoma, median survival times were 6.3 and 5.4 months, respectively ($p = 0.09$; HR: 0.84; 0.49–0.92). However, gefitinib prolonged survival in never-smokers (median survival time [MST]: 8.9 vs 6.1 months; $p = 0.012$) as well as in Asian patients (MST: 9.5 vs 5.5 months; $p = 0.01$) in preplanned subset analyses. Based on these results, the FDA limits the indication of gefitinib to cancer patients who are currently benefiting or have previously benefited from gefitinib treatment or are enrolled in clinical trials as of June 2005.

Gefitinib versus chemotherapy in pretreated advanced NSCLC

Recently, the results of two large Phase III studies were reported (INTEREST and V-15-32). The INTEREST trial compared gefitinib with docetaxel as the second- or third-line therapy in 1466 advanced NSCLC patients with prior treatment of platinum-based chemotherapy [18,69]. Noninferiority of gefitinib in OS was demonstrated (MST: 7.6 vs 8.0 months; HR: 1.020; 95% CI: 0.905–1.150). The one point that should be highlighted in this study is that all of the predictors of efficacy identified in the gefitinib versus placebo studies, including adenocarcinoma, women, Asian and never-smoker, disappear in the comparison with the docetaxel group. The results suggest that these clinical characteristics may be efficacy predictors for docetaxel as well as gefitinib. Gefitinib and docetaxel were equally effective as the second-line therapy for advanced NSCLC patients but gefitinib resulted in an improved quality of life and less toxicity compared with docetaxel. Recently, Douillard *et al.* reported that OS was equally improved with both gefitinib or docetaxel treatments in *EGFR* mutation positive patients compared with *EGFR* mutation-negative patients [69]. On the other hand, PFS was longer with gefitinib than docetaxel in mutation-positive patients [69]. In the V-15-32 trial, however, noninferiority of gefitinib was not demonstrated [19]. The V-15-32 trial, almost identical to the INTEREST trial comparing gefitinib with docetaxel, was a comparative study of 489 patients that was conducted in Japan. The response rate in the gefitinib group was approximately twice as high as in the docetaxel group, but it was impossible to demonstrate noninferiority in OS of gefitinib compared with docetaxel. The survival rate at an early stage, such as less than 1 year, and the CI for therapeutic effects indicated that docetaxel was better than gefitinib. While noninferiority in OS between gefitinib and docetaxel was not demonstrated according to predefined criteria, there was no statistically significant difference in survival between the two arms. This discrepancy in survival between the INTEREST and V-15-32 could be attributable to the smaller patient numbers and imbalances in poststudy treatments in the V-15-32 trial (36% in the gefitinib vs 53% in the docetaxel arm had switched over to the opposite treatment after discontinuation of the study treatment). These two studies established the fact that gefitinib is better tolerated than docetaxel with less toxicities and better quality of life. Recently, Lee *et al.* reported the results of randomized Phase III study (Iressa as Second line Therapy in Advanced NSCLC-Korea [ISTANA]) conducted in Korea [70]. They concluded that PFS was longer with gefitinib compared with docetaxel ($p = 0.04$).

Gefitinib versus chemotherapy as first-line therapy in NSCLC

The result of IPASS has been reported [20]. This large-scale randomized study, which compared gefitinib monotherapy with carboplatin/paclitaxel for previously untreated patients with adenocarcinoma who were never- or light-smokers, was started in April 2004. The results showed improved PFS time in the gefitinib arm; however, the HR was constant over time, initially favoring the carboplatin/paclitaxel arm and later favoring the gefitinib arm, indicating the possibility of gefitinib as the first-line therapy in selected patients. Results of this pivotal trial might establish the role of gefitinib as the first-line therapy in selected patients with advanced NSCLC (Table 3).

Randomized trials currently in progress

At present, the West Japan Oncology Group is conducting a multicenter clinical trial (WJTOG3405) that targets progressive/recurrent lung cancer patients with *EGFR* gene mutations

Table 3. Phase III studies of gefitinib.

Author/study	Treatment arms	Number	ORR (%)	PFS (months)	MST (months)	Comments	Ref.
Chemotherapy with gefitinib in the first line treatment of non-small cell lung cancer							
Giaccone (INTACT-1)	Gem/cis + gefitinib 250 mg	365	51.2	5.8	9.9	Phase III negative trial, corresponding with the TALENT trial	[13]
	Gem/cis + gefitinib 500 mg	365	50.3 (p = NS)	5.5 (p = 0.76)	9.9 (p = 0.46)		
	Gem/cis + placebo	363	47.2	6.0	10.9		
Herbst (INTACT-2)	Pac/carbo + gefitinib 250 mg	345	30.4	5.3	9.8	Phase III negative trial, corresponding with the TRIBUTE trial	[14]
	Pac/carbo + gefitinib 500 mg	347	30.0 (p = NS)	4.6 (p = 0.06)	8.7 (p = 0.64)	Subset analysis of patients with adenocarcinoma who received 90 days' chemotherapy demonstrated statistically significant prolonged survival, suggesting a gefitinib maintenance effect	
	Pac/carbo + placebo	345	28.7	5	9.9		
Kelly (SWOG 0023)	Gefitinib	118	NA	8.3 (p = 0.17)	23 (p = 0.01)	Phase III trial of maintenance therapy after definitive chemoradiation in stage III NSCLC	[68]
	Placebo	125		11.7	35		
Hida (WJTOG0203)	Chemotherapy + gefitinib 250 mg	300	34.2	4.6 (p < 0.001)	13.68 (p = 0.10)	Phase III trial of sequential therapy Superior overall survival time with adenocarcinoma histology in the gefitinib arm (p = 0.03)	[17]
	Chemotherapy alone	298	29.3	4.2	12.89		
Gefitinib versus BSC in the treatment of advanced non-small cell lung cancer							
Thacher (ISEL)	Gefitinib	1129	8.0 (p < 0.0001)	3.0* (p = 0.0006)	5.6 (p = 0.09)	Survival advantage seen in nonsmoking and Asian patients; MST, p = 0.03 by Cox's analysis	[12]
	Placebo	563	1.0	2.6*	5.1		
Gefitinib compared with chemotherapy in the treatment of advanced non-small cell lung cancer							
Douillard (INTEREST)	Gefitinib 250 mg	733	9.10 (p = 0.33)	2.2 (p = 0.47)	7.6 (HR: 1.04)	Effect seen across subgroups: favorable toxicity profile with gefitinib; noninferiority of gefitinib demonstrated	[18]
	Docetaxel 75 mg/m²	733	7.6	2.7	8.0		
Maruyama (V-15-32)	Gefitinib 250 mg	245	22.5 (p = 0.009)	2.0 (p = 0.34)	11.5 (p = 0.33)	Favorable toxicity profile with gefitinib; noninferiority of gefitinib not demonstrated	[19]
	Docetaxel 60 mg/m²	244	12.8	2.0	14.0		

*Time to treatment failure.
†Preliminary (37% maturity).
BSC: Best supportive care; Carbo: Carboplatin; Cis: Cisplatin; EGFR: EGF receptor; Gem: Gemcitabine; HR: Hazard ratio; INTACT: IRESSA NSCLC Trial Assessing Combination Treatment; INTEREST: IRESSA Non-Small-Cell Lung Cancer Trial Evaluating Response and Survival Against Taxotere; IPASS: IRESSA Pan-Asia study; ISTANA: Iressa as Second line Therapy in Advanced Non-Small Cell Lung Cancer-Korea; ISEL: IRESSA® Survival Evaluation in Lung Cancer; MST: Median survival time; NA: Not available; NS: Not significant; NSCLC: Non-small-cell lung cancer; ORR: Overall respone rate; Pac: Paclitaxel; PFS: Progression-free survival; SWOG: Southwest Oncology Group.

Table 3. Phase III studies of gefitinib.

Author/study	Treatment arms	Number of patients	ORR (%)	PFS (months)	MST (months)	Comments	Ref.
Lee (ISTANA)	Gefitinib 250 mg	82	28.1 ($p = 0.0007$)	3.3 ($p = 0.04$)	N/A	Second-line chemotherapy previously received platinum-based chemotherapy; PFS was longer with gefitinib arm ($p = 0.04$)	[70]
	Docetaxel 75 mg/m²	79	7.6	3.4	N/A		
Mok (IPASS)	Gefitinib 250 mg	606	43.0 ($p = 0.0001$)	5.7 ($p < 0.0001$)	18.6‡	Open-labeled, randomized, Phase III previously untreated patients with adenocarcinoma who are never- or light-smokers; improved PFS in the gefitinib arm; PFS favoured pac/carbo initially and then gefitinib, potentially driven by different outcomes according to EGFR mutation status	[20]
	Pac/carbo	606	32.2	5.8	17.3‡		

*Time to treatment failure.
‡Preliminary (37% maturity).
BSC: Best supportive care; Carbo: Carboplatin; Cis: Cisplatin; EGFR: EGF receptor; Gem: Gemcitabine; HR: Hazard ratio; INTACT: IRESSA NSCLC Trial Assessing Combination Treatment; INTEREST: IRESSA Non-Small-Cell Lung Cancer Trial Evaluating Response and Survival Against Taxotere; IPASS: IRESSA Pan-Asia study; ISTANA: Iressa as Second line Therapy in Advanced Non-Small Cell Lung Cancer-Korea; ISEL: IRESSA® Survival Evaluation in Lung Cancer; MST: Median survival time; NA: Not available; NS: Not significant; NSCLC: Non-small-cell lung cancer; ORR: Overall respone rate; Pac: Paclitaxel; PFS: Progression-free survival; SWOG: Southwest Oncology Group.

assigned randomly to a standard treatment (cisplatin plus docetaxel) or a gefitinib-treatment group. It uses PFS as a primary end point. In addition, the North-East Japan Gefitinib Study Group is carrying out a similar clinical trial that targets stage IIIB/IV lung cancer patients assigned randomly into a carboplatin plus paclitaxel treatment or a gefitinib-treatment group and that also uses PFS as a primary end point. The European Organization for Research and Treatment of Cancer are currently testing a Phase III trial of gefitinib or placebo following first-line chemotherapy (EORTC08021) (Table 4).

EGFR in NSCLC

Clinical trial data suggested that gefitinib was more efficacious in patients who were never smokers, female or had adenocarcinoma histology. Since a different 'targeted therapy' (e.g., trastuzumab) was known to be most effective in patients whose tumors had high levels of expression of that drug's target (HER2), an important question was whether responses to gefitinib correlated with levels of EGFR expression [71]. However, analyses of specimens from gefitinib-sensitive and -refractory tumors using immunohistochemistry (IHC) showed no relationship between tumor sensitivity and EGFR expression levels [72–74]. Negative findings regarding the predictive value of EGFR protein expression using IHC in gefitinib-treated patients raised considerable doubt about the role of IHC techniques in patient selection. Recently, Hirsch *et al.* have demonstrated that EGFR immunostaining with the Dako PharmDx kit according to the percentage of cells with positive staining appears to better predict for survival outcome with gefitinib than Zymed antibody according to staining index [75]. With the discovery of EGFR-activating mutations in tumors from most patients who had EGFR TKI-induced tumor responses, skepticism was soon replaced by enthusiasm for molecular profile research in patients treated with EGFR TKIs. There is increasing evidence that EGFR mutations and high *EGFR* gene copy number are associated with higher response rates and longer survival in patients receiving EGFR TKI therapy.

EGFR mutations

In previous studies that investigated the relationship between *EGFR* gene mutations and sensitivity to EGFR TKIs, objective responses were seen in more than 60% of lung cancer patients, with *EGFR* gene mutations receiving EGFR TKI treatment, whereas objective response was seen in only 10% of patients with no mutations (Table 5) [24,76–80]. The response rate of gefitinib of Western NSCLC patients is approximately 10%, much lower than the response rate 20–30% of East Asian patients. This discrepancy may be due to the EGFR mutations [21]. With mutant *EGFR*, the gefitinib response rate of East Asian patients is approximately 60–80%, but goes down to 0–30% in East Asian patients without mutant *EGFR* [60,81]. *EGFR* mutations are mainly present in the first four exons of the gene encoding the tyrosine kinase domain. Approximately 90% of the EGFR mutations are either small deletions encompassing five amino acids from codons 746 through 750 (ELREA) or missense

mutations resulting in leucine to arginine at codon 858 (L858R) [82]. There are over 20 variant types of deletion, for example, larger deletion, deletion plus point mutation and deletion plus insertion. Approximately 3% of the mutations occur at codon 719, resulting in the substitution of glycine to cysteine, alanine or serine (G719X). Furthermore, approximately 3% are in-frame insertion mutations in exon 20. These four types of mutations seldom occur simultaneously. There are many rare point mutations, some of which occur with L858R. Sensitivity of cancers to EGFR TKI was found to be more than 70% in patients with exon 19 and exon 21 mutations. Variations in response rate may arise from different classes of EGFR mutations. Patients with an exon 19 deletion or L858R showed high response rates of 81 and 71%, respectively. By contrast, only approximately 50% of the patients with G719X responded to EGFR TKIs. There have been few reports on insertion mutations associated with clinical effects of EGFR TKIs (Figure 2) [25,59,83–86]. Many investigators have reported that patients with EGFR mutations have a significantly longer survival than those with wild-type EGFR when treated with EGFR-TKIs. However, this point is still controversial because some investigators indicated that patients with EGFR mutations survived for a longer period than those without EGFR mutations even when treated by chemotherapy [87,88].

Table 4. Randomized trials with gefitinib currently in progress.

Study name	Population	Treatment arm	Primary endpoint
WJTOG3405	First-line chemotherapy with EGFR gene mutation	Gefitinib vs cisplatin + docetaxel	PFS
NEJGSG	First-line chemotherapy with EGFR gene mutation	Gefitinib vs carboplatin + paclitaxel	PFS
NCIC BR.19	First-line maintenance after complete resection of stage I-IIIA NSCLC ± adjuvant chemotherapy	Gefitinib vs placebo	OS
EORTC08021	First-line maintenance for advanced NSCLC in patients without disease progression after chemotherapy	Gefitinib vs placebo	OS

EGFR: EGF receptor; NCIC: National Cancer Institute of Canada; NEJGSG: North-East Japan Gefitinib Study Group; NSCLC: Non-small-cell lung cancer; OS: Overall survival; PFS: Progression-free survival; WJTOG: West Japan Thoracic Oncology Group.

EGFR secondary mutations & resistance against EGFR TKIs

Another major issue is that nearly all patients who respond initially to EGFR TKIs later develop drug resistance (Figure 3). The effective period of EGFR TKI varies from 2–4 months to more than 2 years. It has been reported that, in some patients with such acquired resistance, in addition to the original deletion and L858R mutations that elevate sensitivity to EGFR TKIs, an extra secondary mutation occurs with the threonine at codon 790 being changed to a methionine (T790M) [89]. Tumors with T790M are highly resistant to reversible TKIs, such as gefitinib or erlotinib. However, the T790M mutant kinase remains sensitive to irreversible inhibitors, including CL-387,785, EKB-569, and HKI-272 [89–93]. Although the substitution in EGFR with a bulky methionine has been thought to cause resistance by steric interference with binding of TKIs, including gefitinib and erlotinib, Yun *et al.* have reported that the T790M mutation is a 'generic' resistance mutation that will reduce the potency of any ATP-competitive kinase inhibitor (T790M substitution confers resistance by increasing the affinity for ATP) and that irreversible inhibitors overcome this resistance simply through covalent binding, not as a result of an alternative binding mode [94]. Recently, Engelman *et al.* reported that amplification of the *MET* gene is another mechanism of acquired resistance to EGFR TKIs [95,96]. With the use of a 1000-times resistant cell line, HCC827GR, established by exposing it to increasing concentrations of gefitinib, the authors found that phosphorylated forms of MET, ERBB3 and EGFR remain after gefitinib treatment and that the *MET* gene is amplified. Inhibition of *MET* signaling restored the cells' sensitivity to gefitinib. *MET* amplification was also detected in four of 18 (22%) clinical specimens

Table 5. *EGFR* mutations versus wild-type *EGFR* related to response rate, progression-free survival and overall survival in patients treated with gefitinib.

Study	Patients (n)	Mutation (%)	Response rate (mutation/wild-type; %)	PFS (mutation/wild-type; months)	OS (mutation/wild-type; months)	Ref
Cappuzzo *et al.*	89	19	54/5	9.9/2.6	20.4/8.4	[24]
Cortez-Funes *et al.*	83	12	60/9	12.3/3.6	13.0/4.9	[76]
Han *et al.*	90	19	65/14	21.7/1.8	30.5/6.6	[77]
Takano *et al.*	66	59	82/11	12.6/1.7	20.4/6.9	[78]
Mitsudomi *et al.*	59	56	83/10			[79]
Taron *et al.*	68	25	94/13		–/9.9	[80]

OS: Overall survival; PFS: Progression-free survival.